

Design of a Patient-Specific Knee Osteotomy Plate

A workflow for in-house design of a patient-specific fixation device in malalignment surgery with 3D-technology in patients for whom off the shelf solutions do not fit.



Author: Laura Miessen

Master Thesis Technical Medicine

September 2023

University of Twente
Technical Medicine – Medical Imaging and Intervention
M3 Clinical Internship

Universitair Medisch Centrum Utrecht
Orthopaedics Department & 3D-Lab

Graduation Committee

Chairman	prof. dr. ir. N.J.J. Verdonschot
Medical supervisors	dr. R.J.H. Custers dr. N. van Egmond
Technical supervisor	ir. E.E.G. Hekman
Daily supervisor	H.C. Nguyen MSc
Process supervisor	E.M. Walter MSc
External member	prof. dr. H.B.J. Karperien

UNIVERSITY OF TWENTE.



A. Abstract

Background

In patients with rare bone deformities, the abnormal geometry of the bone and altered biomechanics raise some technical challenges when it comes to fixation with a generic plate after an osteotomy. Patients suffer from soft tissue irritation, procedures have longer operation times and mechanical safety may not be assured. This study aimed to develop a workflow for *in-house* design of a patient-specific plate in malalignment surgery with 3D technology in patients for whom *off the shelf* solutions do not fit, and to evaluate the mechanical safety and feasibility.

Methods

Design requirements and a design workflow are based on literature, measurements in generic plates, and estimations of the required plate thickness in a Finite Element Analysis, to ensure mechanical safety. The feasibility is evaluated based on a virtual validation of the design workflow in 5 patients, and exploration of the manufacturing process, costs and risks.

Results

Design requirements and a workflow are proposed for designing patient-specific plates. The required thickness depending on the curve of the patient-specific plate is determined, varying from 2.9 to 5.9 mm. The virtual validation demonstrated that most of the design requirements were met, except for the 2 mm limit for the plate-bone gap, which was exceeded in one out of five patients. Milling the plate was considered preferable, and additional costs were estimated around 3000 euros for the manufacturing process, along with increased labour costs.

Conclusion

A workflow was successfully developed for *in-house* design of a patient-specific osteotomy plate in patients for whom *off the shelf* solutions do not fit. A first estimation was made of the required thickness of the plates to ensure mechanical safety. The workflow could be feasible when the benefits outweigh the costs. Further research is recommended to conduct a more comprehensive cost-benefit analysis, and to determine the optimal balance between plate-bone fitting and the complexity of the plate shape.

Keywords: Knee osteotomy, Patient-specific plate, Bone deformities, Design workflow, In-house design

B. Abbreviations

CAD	Computer-aided design
CT	Computed tomography
DFO	Distal femur osteotomy
DLO	Double level osteotomy
FEA	Finite element analysis
HKA	Hip–knee–ankle
HTO	High tibial ostomy
IFM	Interfragmentary movement
ISO	International Standardization Organization
K-wire	Kirschner-wire
MDR	Medical Device Regulation
MED	Multiple epiphyseal dysplasia
MTCP	Medical Technology and Clinical Physics
OA	Osteoarthritis
PSI	Patient-specific instrument
SLS	Selective laser sintering
SED	Spondyloepiphyseal dysplasia
STEP	Standard for the Exchange of Product
STL	Stereolithography
TOKA	Tailored Osteotomy for Knee Alignment
UMCU	University Medical Center Utrecht
WLR	Whole leg radiographs
3D	Three-dimensional

Contents

A. Abstract.....	1
B. Abbreviations.....	2
1. General introduction.....	4
2. Competitive Product Analysis	9
3. Design	12
3.1 Product Specifications	12
3.2 Statement of Requirements.....	14
3.3 Design Workflow of the Basic Shape	15
3.4 Mechanical Safety	19
3.5 Discussion: Design	25
4 Validation	28
4.1 Validation Design Workflow.....	28
4.2 Manufacturing and Costs	31
4.3 Risk Analysis	33
4.4 Discussion: Validation.....	35
5 General Discussion	37
6 General Conclusion	39
7 References	40
Appendix A. Background Literature Design Requirements.....	44
Appendix B. Theory Simple Bending of a Beam	46
Appendix C. Virtual Validation Analysis	47
Appendix D. Risk Analysis: Potential Modes of Failure.....	49

1. General introduction

With a prevalence of 23 per 1,000 persons a year, knee osteoarthritis (OA) is the most common joint disorder in the Netherlands¹. Knee OA is diagnosed when the cartilage in the knee joint gradually wears away, affecting all of the tissues in the joint and causing detectable changes in tissue architecture, its metabolism, and function². Patients experience persisting pain, limited morning stiffness, and reduced function³. OA is a progressive, heterogeneous, and multifaceted disease with multiple molecular and clinical phenotypes. Both intrinsic and extrinsic risk factors promote its development, including genetic factors, age, sex, obesity, and lifestyle.⁴ A recent systematic review suggests six phenotypes characterized by unusual inflammation inside the knee joint, chronic pain, systemic metabolic disorders including obesity, changes in bone and cartilage metabolism in the knee, minimal joint disease with minor symptoms and discomfort, and malaligned biomechanics⁵.

Knee malalignment is categorized across three distinct planes: the coronal plane, the sagittal plane, and the axial plane. Coronal plane joint malalignment of the lower extremity occurs when the legs are in valgus or varus (Figure 1). The hip–knee–ankle angle (HKA), defined as the angle between the mechanical axes of the femur and tibia, is used to measure the lower limb alignment⁶. In healthy adults with a neutral alignment, HKA is between 1.0° and 1.5° of varus⁷. Normally, approximately 60% of the weight-bearing force is on the medial tibiofemoral compartment and 40% on the lateral compartment⁸. When the mechanical axis is shifted in valgus or varus position, either the medial or the lateral compartment is overloaded, increasing the risk of progression of knee OA^{9,10}. Sagittal plane deformity of the distal femur and/or proximal tibia may cause flexion and extension deficits and the tibial slope influences the knee stability (Figure 2)¹¹. Axial plane deformities include tibial torsion, responsible for patellofemoral instability¹², and femoral neck anteversion, associated with early hip OA¹³.

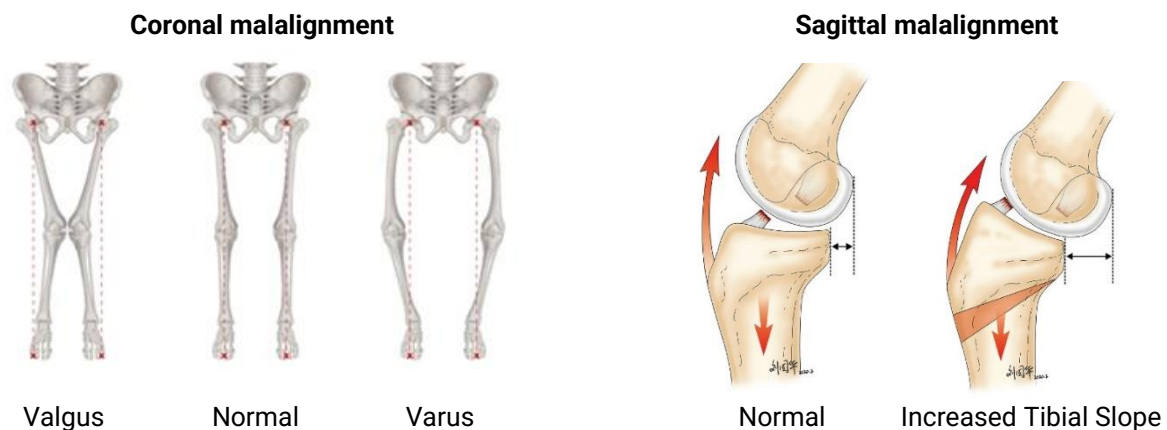


Figure 1: Illustration of coronal malalignment. Valgus and varus with the mechanical axis of the lower limb represented by the red dotted line. Adapted from original image¹⁴.

Figure 2: Illustration of sagittal malalignment: An increased tibial slope results in knee instability after anterior cruciate ligament injury. Adapted from original image¹⁴.

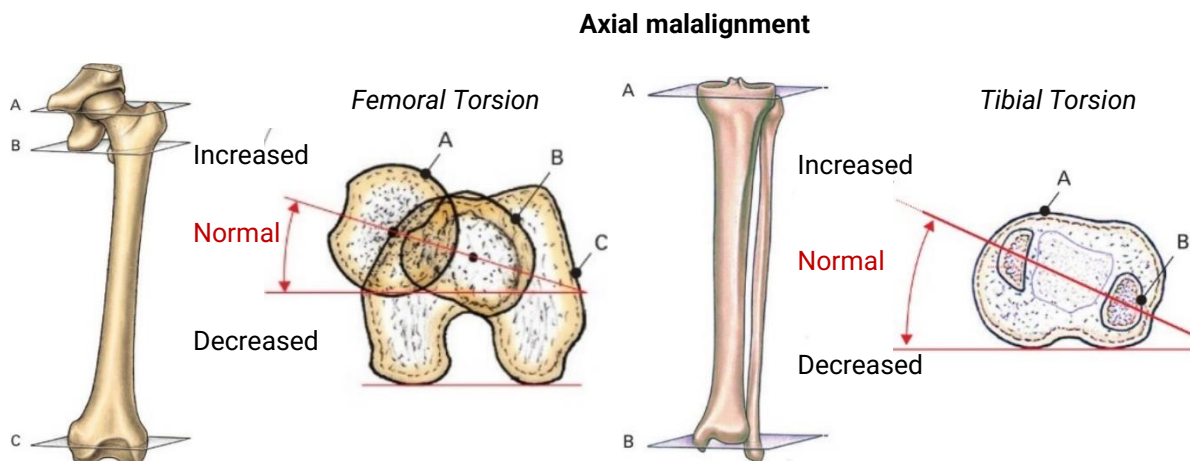


Figure 3: Illustration of axial malalignment. Rotation in the femur or in the tibia. Adapted from original image¹⁵.

The first line of treatment for knee OA due to malalignment is conservative management. The most important aim is to provide symptomatic relief and to avoid or delay the need for surgical intervention. Conservative treatment options include exercise, weight loss, pharmacological agents, knee bracing, and orthotics¹⁶. The end-stage option for malalignment is partial or total knee replacement, which is a non-reversible surgery. With a knee replacement, the natural joint structures are removed and replaced with a prosthesis. Approximately 20% of knee replacement patients are unsatisfied with their knee arthroplasty¹⁷, with even higher rates of revision and greater levels of dissatisfaction amongst patients under sixty years old¹⁸.

A joint preserving surgical treatment option in patients is a corrective osteotomy. The goal is to shift the mechanical axis from the injured knee compartment to the healthy knee compartment, reducing the load in the painful compartment¹⁹. Osteotomies can be classified into several techniques, high tibial ostomy (HTO), distal femur osteotomy (DFO), or a combination of both, called a double level osteotomy (DLO). Both HTO and DFO can be performed using open wedge or closed wedge technique on the medial side or the lateral side (Figure 4A). The indication for a technique depends on the location of the deformity and the size of the correction²⁰⁻²². A correction of valgus or varus in the coronal plane can be combined with a slope correction in the sagittal plane (Figure 4B). Slope corrections are performed to address cruciate ligament pathology and reconstruction failure or to treat meniscal or cartilage pathology²³. A derotation osteotomy in the axial plane can be performed in either the distal femur to address anterior knee pain with patellofemoral instability, or in the tibia in case of excessive tibial torsion¹¹ (Figure 4C).

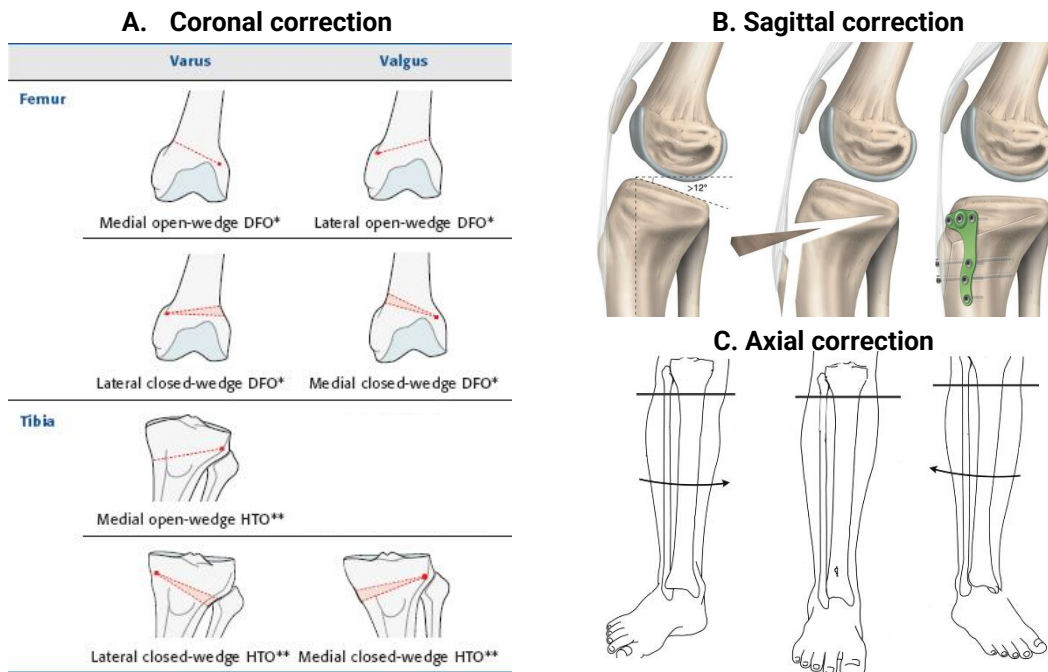


Figure 4: The various types of osteotomies performed in the UMCU. A) In the coronal plane the distal femur (DFO) and the high tibial osteotomies (HTO). The red lines show the cutting planes, red areas are removed in closed wedge osteotomy. B) In the sagittal plane a closed wedge tibial slope correction and c) in the axial plane derotation osteotomies with the cutting lines in black. Adapted from original images²⁴⁻²⁶.

Due to recent advancements in innovative technologies, there is a growing potential to perform more complex osteotomies in patients with rare bone deformations caused by conditions such as achondroplasia, dysplasia, or trauma. Osteotomies in these patients can prevent premature development of OA, and improvements of pain and function have been consistently reported^{27,28}. However, the procedure can be technically challenging due to the bone deformities, small bone caliber, ligament laxity, and soft tissue contractures²⁹. Therefore, the University Medical Center Utrecht (UMCU) has introduced a workflow using novel three-dimensional (3D) technology for pre-operative planning and intraoperative guidance (Figure 5). The corrective coronal plane angle is calculated based on antero-posterior weight bearing whole leg radiographs (WLR), as it is for non-complex patients. Additionally, a more extensive deformity analysis is performed in the segmentation of a computed tomography (CT) scan, measuring the rotations in the axial plane and the sagittal slope. Based on the 3D planning, a patient-specific instrument (PSI) can be designed, functioning as an intraoperative drill and saw guide. Previous studies have reported accurate correction of coronal and sagittal angles with the application of a PSI^{30,31}.



Figure 5: Current 3D workflow in the UMCU for knee osteotomy in patients with bone deformities.

While the innovative techniques have expanded the scope of osteotomies for patients with rare bone deformities, a challenge emerges for fixation of the femur or tibia. The PSI is designed to fit one of the generic plates of ActivMotionS (Newclip Technics, Haute-Goulaine, France). A wide

range of plates anatomically contoured are available to fit the proximal curvature and metaphyseal slope, and the design and positioning are adapted to the knee biomechanics of the average patient³². However, the abnormal geometry of the bone and altered biomechanics raise some technical challenges when it comes to plate fixation. Due to changes in knee joint biomechanics and the practical limitation of not always being able to place all screws of a generic device, mechanical safety is not assured³³. Additionally, an abnormal metaphyseal slope or proximal curvature may introduce a plate-bone gap (Figure 6A), increasing the risk of soft tissue irritation. In a clinical study using a generic plate for high tibial osteotomy, 40.6% of the patients suffered from local soft tissue irritation, which necessitated implant removal³⁴. Furthermore, clinical experience shows that osteotomy procedures involving bone deformities typically require longer operation times, as it takes time to find the best position of the generic plate when the shape does not actually fit the bone.

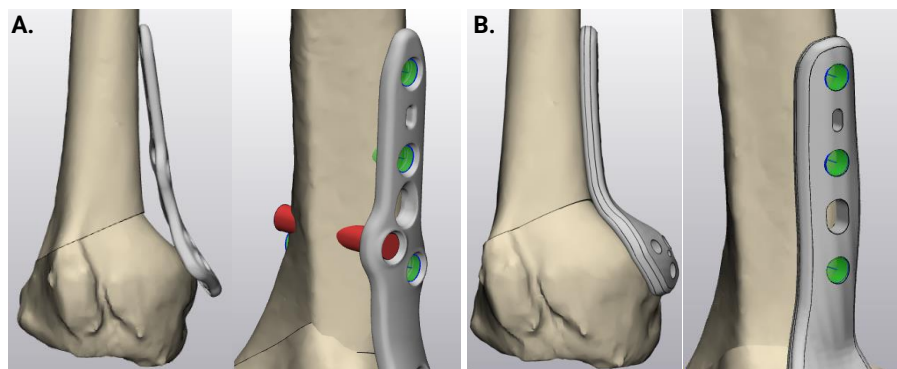


Figure 6: Representations of fixation in two patients with skeletal dysplasia using a) a generic osteotomy plate, introducing a plate-bone gap and screws cannot be placed, and b) using a patient-specific, fitting plate of which all screws can be placed.

It has been hypothesized that the use of a patient-specific fixation device might minimize soft tissue irritation, by minimizing its profile and optimize the shape to the patient's anatomy. Plate design based on individual geometry offers the capability to match the surface of the patient's proximal tibia or distal femur (Figure 6B). When the pre-operatively determined position and orientation are embodied in the surgical guide and fixation device, the surgical procedure can be simplified with reduced surgery time³⁵.

The function of a patient-specific fixation device is to adequately connect and stabilize the bone parts, while stimulating bone growth. Wolff's law states that bone tissue adapts to the mechanical demands placed upon it³⁶. Bone subjected to loading or stress will regenerate and bone not subjected to stress will atrophy. An implant that is much stiffer than bone demonstrates an unphysiological redistribution of force transmission at the interface resulting in reduction in bone density, which is referred to as stress shielding.³⁷ A combination of transverse and axial interfragmentary movement (IFM) between 100 and 200 μm can stimulate callus formation at the fracture site^{38,39}. Fracture site instability prevents bone callus formation⁴⁰, and increases plate stress and potential failure³⁸. Therefore, a balance of a stable fixation that allows for appropriate IFM is crucial to support successful bone healing and reduce the risk of mechanical failure.

The aim of this research is to develop a workflow for *in-house* design of a patient-specific fixation device in malalignment surgery with 3D technology, for patients for whom *off the shelf* solutions do not fit, and to evaluate the mechanical safety and feasibility.

More specifically, the objectives of this thesis are:

1. To set up design specifications, requirements and a design workflow for the fixation device.
2. To determine the required thickness depending on the curve of the plate in a Finite Element Analysis (FEA), aiming to achieve mechanical safety similar to a generic plate.
3. To perform a virtual validation of the design workflow on five patients.
4. To explore the manufacturing process, costs, and risks.

Chapter 2 examines the significance of a novel design by exploring currently available alternatives discussed in literature in a competitive product analysis. **Chapter 3** describes the design process of the plate, covering aspects such as product specifications, design requirements, design of the basic shape, and determining the required thickness in a FEA. **Chapter 4** includes a validation of the workflow in five patients and exploration of the manufacturing process, costs and risks in accordance with the design. The mechanical safety, feasibility, and future perspectives are evaluated in the general discussion in **Chapter 5**. Finally, a general conclusion is described in **Chapter 6**.

The design workflow in this study is focused on designing a closed wedge DFO plate, as clinical experience with such plates shows a high incidence of a poor fit and soft tissue irritation. However, the design principles and general workflow can be applied to the design of all patient-specific osteotomy plates.

2. Competitive Product Analysis

Competitive products for a patient specific fixation device have been analyzed in literature. A framework for development of personalized 3D implants has already been established and implemented in the UMCU (Figure 7) and an ISO 13485 certification has been obtained for the *in-house* quality management system⁴¹. The aim of the competitive product analysis is to highlight opportunities and challenges of design choices of the new device, to explore alternatives. Three lines of research on patient-specific plate designs were selected and described here, and post-processed bending was considered as an alternative for patient-specific plate design.

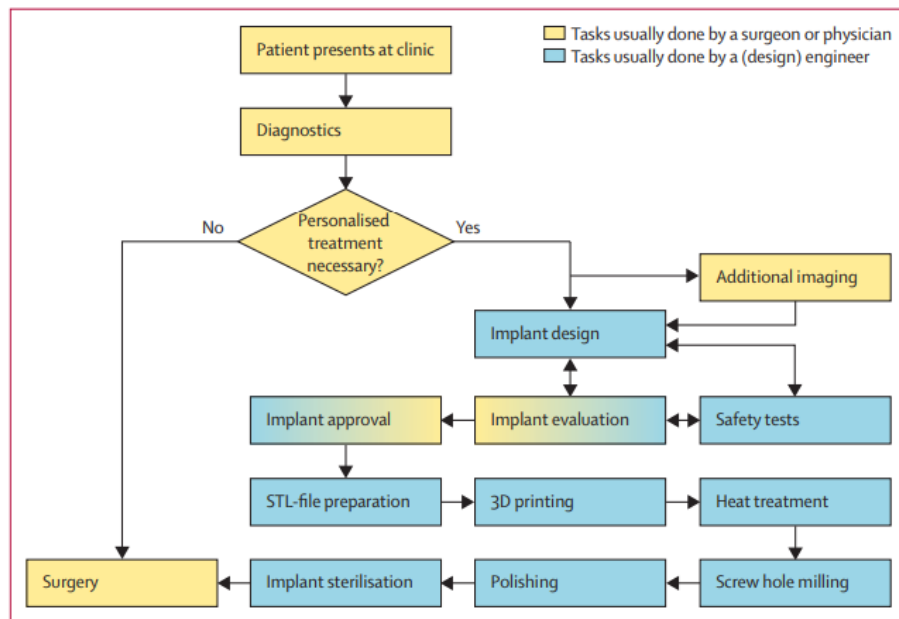


Figure 7: Workflow for development of personalized 3D implants in the UMCU by Willemsen et al.⁴¹

Patient-specific knee plates

In previous research, the 3D lab in Groningen introduced a personalized approach for acetabulum fracture treatment. The patient-specific implant fitting facilitated proper fracture reduction and yielded good clinical outcomes.^{42,43} Their most recent feasibility study⁴⁴ described the *in-house* development and implementation of a patient-specific drilling guide for medial tibial plateau fracture surgery (Figure 8a). A workflow was proposed that facilitates proper fracture reduction, tibial alignment, and accurately placed screws by using custom-made osteosynthesis plates with drilling guides. The workflow consisted of CT-scanning, 3D reconstruction, pre-operative planning, 3D design of the plate and surgical guide, production, sterilization, and clinical application in human cadavers. The plates were made of a medical grade titanium alloy by milling using a 5-axis milling machine. The challenges highlighted were that the innovative workflow required substantial resources, including a dedicated team, validated software packages, and an osteosynthesis plate production facility. These resources are all available in the UMCU. The associated costs for these resources were not part of the feasibility study.

The research group at the University of Bath led by MacLeod has published several articles about a patient-specific high tibial osteotomy plate (Figure 8b). In 2018, MacLeod et al.³⁸ analyzed the effect of plate design and bridging span on the performance of the custom made plate. A FEA showed that the optimized plate design produced plate stress similar to that in the TomoFix plate for short and long bridging spans while substantially reducing high strain regions within the bone. In 2021⁴⁵, they published an in-silico trial, virtually performing an HTO with either a generic or a personalized plate and they compared the plates using a FEA. The personalized plate showed no increased risk of failure, whilst being more mechanically efficient and less stiff. IFM was similar for both types of devices, indicating that there is no difference in the stability of the osteotomy. In the most recent report in 2022³⁵, a cadaver study using the custom-made titanium alloy plate and a personalized surgical guide is described. The study demonstrated a higher accuracy of the correction angle compared to conventional or other patient-specific methods available, suggesting the method can potentially improve the accuracy of osteotomy correction. The plate developed by the research team has been patented under the product name TOKA (Tailored Osteotomy for Knee Alignment) by Orthoscape (Orthoscape, 3D Metal Printing Ltd, University of Bath, Innovation Centre, Bath, UK). The company has obtained ISO13485 certification for their quality management system to produce the tibial plates and partnered with hospitals to obtain regulatory approval for the initial clinical trials. The product is not available on the market yet.

A novel method for designing a HTO plate was suggested by Kanagalingam et al. (2022)⁴⁶ by applying a generative design (Figure 8c). Generative design is the process of using parameters and goals in an AI algorithm to quickly explore thousands of design variants to find the best solution. In general, products based on generative design have reduced weight, improved performance, increased efficiency and customized product development⁴⁷. The design study includes detailed design requirements of the HTO plates for manufacturing by electron beam powder bed fusion of Ti-6Al-4 technology, including the post-processing steps required to transform the digital design into a physical part. The application of generative design has allowed concept designs to be undertaken simultaneously considering patient factors, surgical planning parameters and patient-specific biomechanics with the aim to reduce plate stiffness and profile on soft tissue. However, the authors mentioned that the methods of design, fabrication, and post processing are advanced, suggesting a significantly higher cost per plate for material, time and labor, as compared to the clinical standard.⁴⁶

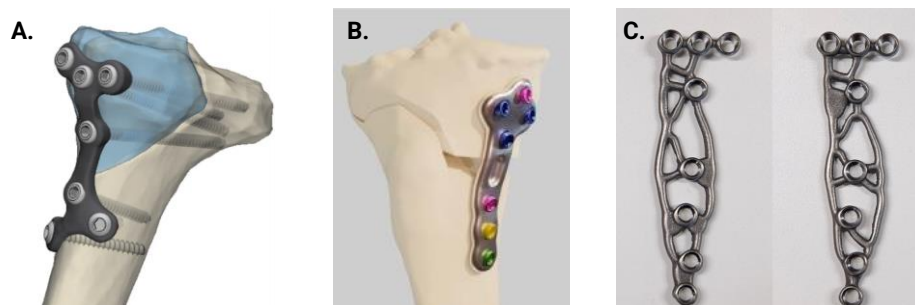


Figure 8: Tibial patient-specific plates designed by a) 3D lab Groningen⁴⁴, b) MacLeod et al.³⁵ and c) Kanagalingam et al.⁴⁶.

Post process bending

An alternative for patient-specific osteotomy plates is bending of generic plates, as it is cost-effective and easily available. This technique was conventionally used intra-operatively with titanium plates in conventional mandibular orthopedic procedures. However, the manual contouring process is time consuming, technique-demanding, and could adversely affect the precise location of bone segments⁴⁸. An additional risk is that repeated bending can lead to poor fatigue performance of surgical plates, as bending may create stress concentrations⁴⁹.

Conclusion

The competitive product analysis has highlighted several opportunities for patient-specific plate design. The feasibility of *in-house* patient-specific design was demonstrated by the 3D lab in Groningen. MacLeod et al. demonstrated the potential of achieving a high correction angle accuracy and no increased failure risk when employing patient-specific osteotomy plates. However, the challenges highlighted in their safety study led to the decision to explore an alternative method for ensuring mechanical safety in this research. A potential future alternative is the TOKA plate, although the product is not available on the market yet. Generative design and post-processed bending were considered unviable alternatives due to time-constraints, complexity, or safety risks.

3. Design

3.1 Product Specifications

Intended purpose

The function of the patient-specific osteotomy plate is to adequately connect and stabilize the distal and proximal femoral bone, while stimulating bone growth. The design is optimized to fit the patient's anatomy, especially patients with rare bone deformities for whom *off the shelf* solutions do not fit.

A patient-specific fixation device requires additional steps relative to the current clinical workflow for patients with bone deformities scheduled for an osteotomy (Figure 9). The initial steps of medical imaging and pre-operative planning remain unchanged. The treating surgeon requests a CT-scan in addition to the whole leg radiograph. CT-scans are acquired using Philips iCT scanner or Philips Brilliance 64 (Philips Medical Systems, Best, The Netherlands). A specialist from the 3D lab conducts pre-operative planning, starting with segmentation in Mimics 25.0 (Materialise, Leuven, Belgium), to create a 3D bone model of the lower limb. The bone models are transferred to 3-Matic 17.0 (Materialise, Leuven, Belgium) to perform deformity analysis and virtually conduct the osteotomy using a generic plate for fixation. The surgeon and 3D specialist collaborate to determine if the patient is eligible for a generic plate, meaning all screws can be placed in the pre-operative planning and the plate-bone distance does not exceed the limit. If not, the 3D specialist designs a patient-specific osteotomy plate according to the guidelines outlined in Section 3.3. The manufacturing process is then outsourced to an external company specialized in medical devices and implants. It is important to note that the legal manufacturer of the patient specific plate is the department Medical Technology and Clinical Physics (MTCP) within the UMCU. A PSI is designed by the 3D specialist, following the current protocol and printed *in-house* by the MTCP in polyamide-12 with a selective laser sintering 3D printer. The orthopedic surgeon performs the osteotomy procedure with guidance of the PSI and fixates the bones with the patient-specific osteotomy plate.



Figure 9: Proposed clinical 3D workflow in the UMCU for knee osteotomy with a patient-specific plate. Additional steps to the current workflow are colored in orange.

Intended users

The osteotomy and fixation with the patient-specific plate is performed by an orthopedic surgeon in the UMCU, specialized in joint preserving knee treatments. The plate is designed by a specialist from the medical 3D lab in the UMCU, in close cooperation with the orthopedic surgeon. The MTCP functions as the legal manufacturer and fulfills an advisory and supervisory role concerning design and safety aspects.

Intended patient group

The design workflow is focused on designing a closed wedge DFO plate, as clinical experience shows a high incidence of a poor fit and soft tissue irritation. Patients are eligible for a patient-specific closed wedge DFO plate if they meet the following inclusion criteria:

- Eligible for a closed wedge DFO.
- Under treatment at the University Medical Center Utrecht.
- Manifest bone deformity of the femur. Possible causes include achondroplasia, multiple- or spondyloepiphyseal dysplasia (MED or SED) or trauma.
- The generic plate does not fit, meaning:
 - 1 or more screws cannot be placed, and/or
 - the maximum plate-bone distance > 10 mm.

The plate-bone distance is defined as the distance between the cortex and the external boundary of the plate. This should not be confused with the plate-bone gap, wherein the plate's thickness is not included. The established threshold of 10 mm corresponds to the distance at which impingement of the tractus iliotibialis for lateral DFO or the vastus medialis for medial DFO is expected. This estimation is a rough assessment provided by two orthopedic surgeons specialized in osteotomies.

Quick scan

The quick scan serves as an initial assessment of the patient-specific plate, and is a mandatory component of the UMCU's quality management system.

Table 1: Overview of product features, with the category applicable to the device highlighted in bold

Feature	
Risk assessment	[Very low/ Low /Medium/High]
Design complexity	[Low/ Medium /High]
Frequency of clinical usage	[Daily/Weekly/ Monthly /Yearly]
Presence of electronics	[Yes/ No]
Patient-specific device	[Yes/ No]
Invasive use/direct patient contact possible	[Yes/ No]
Classification	[I, IIa, IIb, III]

3.2 Statement of Requirements

Most design requirements are based on measurements obtained from generic certified plates. Adjustments to these measurements following from patient-specific aspects are supported with prior literature, investigating the effects of design requirements on rigidity, IFM, stress distribution, stress shielding, static loading failure, and fatigue failure, detailed in Appendix A. The closed wedge DFO plate must meet the following requirements:

Screws and pins

Type and number of screws and pins

- 6 locking screws: 3 in the proximal fragment, 3 in the distal fragment ^{39,50-54}
- 1 compression screw proximal to the wedge in an oblong ramp hole parallel to the shaft axis ⁵⁵
- 2 Kirschner (k-)wires: 1 proximal to the osteotomy in an oblong hole and 1 distal to the osteotomy in a round hole for temporarily fixation

Screw positions

- No interference with the osteotomy plane or knee joint⁵⁶
- The distance between the centers of the proximal screw holes is minimally 10 mm^{32,36,51,56}
- Proximal screws are oriented perpendicular to the shaft axis, parallel to each other ^{52,57,58}
- Distal screws are oriented in divergent direction⁵⁹ and centered around the most heavily loaded region indicated by the mechanical axis ^{32,60,61}
- The bridging span, defined as the distance between the centers of the screws on either side of the osteotomy line, is 25 mm ± 1 mm ^{32,38,51,52,62}

Plate

Shape

- The distance between the center of the screws and the edge of the plate is at least 6 mm ³²
- The plate-bone gap is limited to a maximum of 2 mm at distal and proximal part measured in the virtual osteotomy during pre-operative planning ^{63,64}
- The edges of the plate and screw holes are rounded ³²
- A smooth curve bridges the step at the level of the osteotomy, based on the offset and the angle of the distal part ⁵⁹

Thickness and strength

- The stress in the plate is similar to, or smaller than, the stress in a generic plate under the same loading
- Depending on the curve of the plate in sagittal direction, the required thickness is determined in heatmap derived from a FEA (Section 3.4)
- Material of the plate is Ti6Al4V, manufactured according to the ISO 13485 requirements

3.3 Design Workflow of the Basic Shape

A workflow is presented to design a patient-specific plate for closed wedge DFO that meets the statement of requirements described in the previous section. The workflow includes the positioning of the screws, shaping of the plate, and applying thickness depending on the longitudinal curve of the plate.

Standard screw configuration

The standard screw and pin formation for the proximal part consists of three locking screws, one compression screw, and one k-wire. The locking screws and compression screw are aligned parallel to each other, maintaining a 10 mm spacing between their centers. Notably, the most proximal screw is positioned at 16 mm, and the oblong screw hole is situated between these screws. The distal locking screws are inserted at varying distances from 9 to 11 mm from one another, oriented in divergent direction as measured in generic plates. The distal k-wire is inserted at the center of gravity of the three distal screw, aligning on the average direction of the three distal screws.

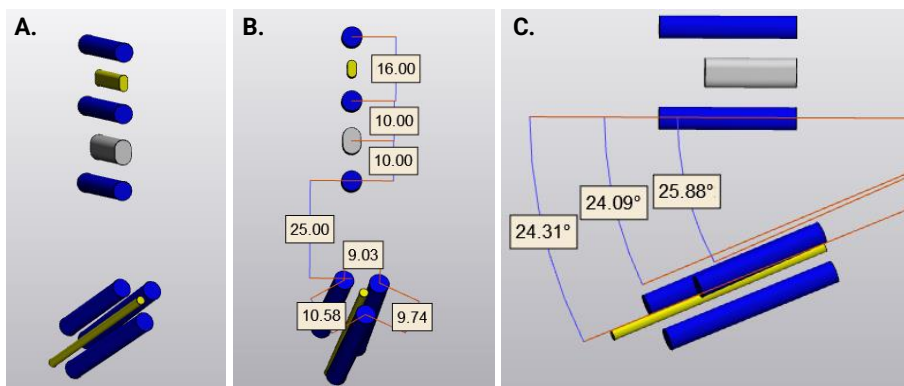


Figure 10a. The standard screw configuration with the locking screws in blue, the compression screw in grey and the k-wires in yellow. Measurements are included of b) the distances between the screw and c) the head-shaft angles.

Patient-specific screw position

The standard screw configuration and virtual post-operative bone model, resulting from the pre-operative planning according to the current workflow in the UMCU, are imported in 3-Matic (Materialise, Leuven, Belgium) (Figure 11A). The proximal and distal femur parts are merged and wrapped. A cylinder is created, fitting the marked shaft of the distal femur. All screws are positioned so that the proximal screws are perpendicular to the shaft, by aligning a plane through the centerlines of the proximal screws to a plane through the centerline of the shaft and the desired point of insertion of the proximal screws (Figure 11B). The distal location of all screws can be adjusted by translating them as a set in direction of the shaft cylinder. The entrance of all screws can be adjusted by rotation around the shaft cylinder. The direction of the distal screws can be adjusted by rotating around the shaft axis with the point of rotation at the head of the round k-wire, aiming for an orientation through the mechanical axis, without interference with the cutting plane or knee joint (Figure 11C).

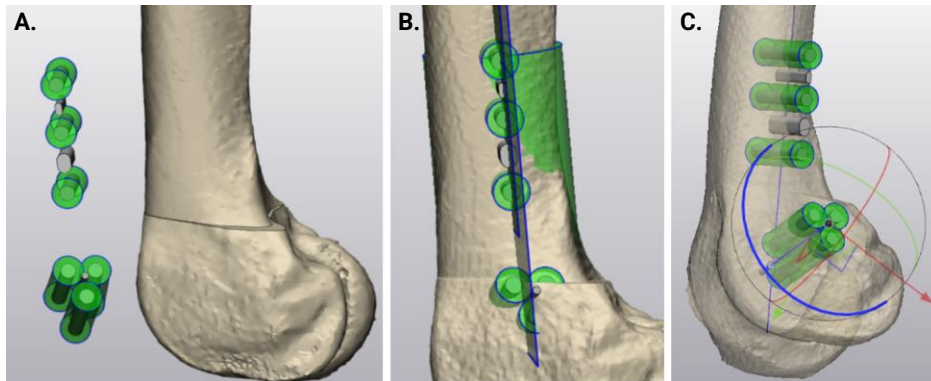


Figure 11. Positioning the screws by a) importing the standard formation, b) moving the screws to the shaft of the femur and c) adjusting screw orientation.

Required plate shape

The surface of the plate is constructed by a curve indicating the outline of the plate and one or multiple sketches over the longitudinal axis of the plate serving as guidelines for the middle part. The outline curve is a smooth, closed curve, attracted to the femur, at 6 mm to the center of the screws indicated by the analytical cylinders (Figure 12A). The part over the step caused by the closed wedge is replaced by a new, smooth, unattached, open curve bridging the step (Figure 12B). The curves are connected, closed, and the result is smoothed. The guideline over the longitudinal axis is a sketch, created in a plane through the middle proximal screw and the most distal screw. The intersection of the femur and the outline curve are imported in the sketch. A smooth spline is created over the femur between the outline curve (Figure 12C). A surface is constructed with the curve and sketch as guiding lines. With part comparison analysis, it can be verified that the distance between surface and the femur at the proximal and distal ends is within a range of 2 mm (Figure 12D). If the distance is larger, additional longitudinal sketches can be created to construct the base surface.

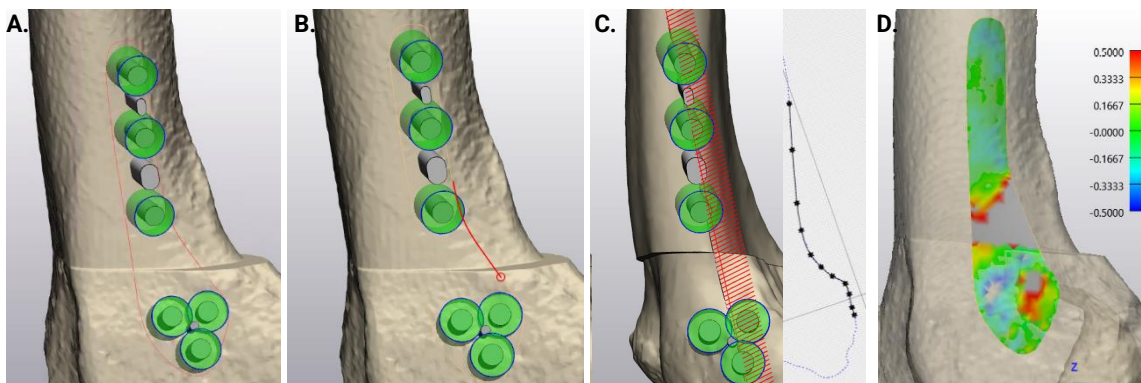


Figure 12. Construction of the plate by a) a curve around the screws with b) smooth curves bridging the step and c) a longitudinal sketch. d) The distance between the femur and constructed surface is checked.

Adaptation to parameterized shape

Depending on the longitudinal curve of the plate, the required thickness can be derived from the heatmap, given in Section 3.4. The longitudinal curve is described by two variables: the offset and distal angle (Figure 13AB). The offset is the distance over the bridging span perpendicular to the proximal axis. The offset is measured in the longitudinal sketch in three steps (Figure 13C). First, a line is drawn along the cortex of the diaphysis. Then, the 25 mm bridging span is measured from the proximal screw closest to the osteotomy along the diaphysis line. Finally, a line from the end of the bridging span, perpendicular to the diaphysis line to the curve of the plate indicates the offset. The distal angle is the angle between the axis along the proximal part and axis along the distal part of the plate. The distal angle is measured between the diaphysis line and a line from the distal end of the bridging span to the distal end of the plate.

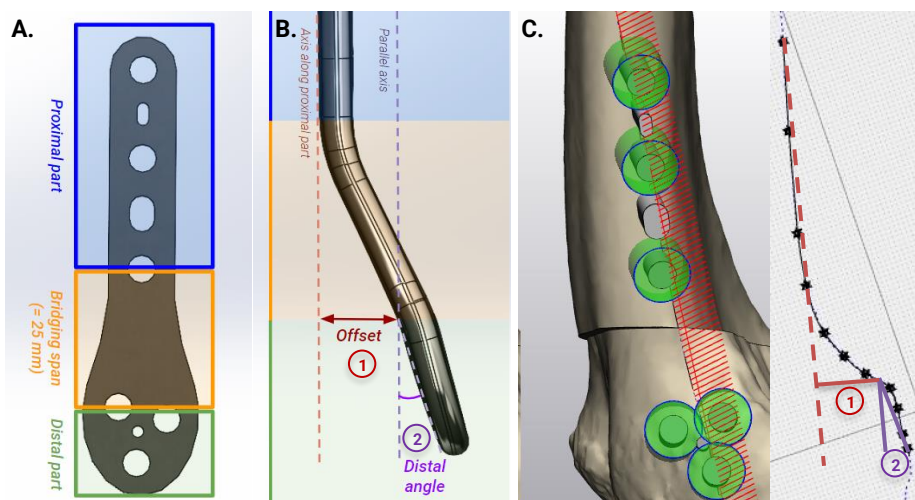


Figure 13ab: Definition of the longitudinal curve defined by the offset and distal angle and c) how to measure the parameters in the design workflow.

Surface to solid body

The base surface is given a uniform thickness with straight boundaries in multiple steps. A duplicate of the base surface, colored red, is moved in direction of the proximal screws. The side surface of the solid body that is created shapes the boundaries of the proximal part of the plate. Another duplicate of the base surface, colored blue, is then moved in the direction of the round k-wire, shaping the boundaries of the distal part. The boundaries of the distal part are formed, moving a blue duplicate in direction of the round k-wire. At the intersection of the red and blue solid bodies, a plane is created. The red and blue plates are both cut by the plane (Figure 14A). The red proximal end and the blue distal end are merged and form the boundaries of the plate (Figure 14B). Then, a third duplicate of the base plate is given a uniform offset of the required thickness, derived from the heatmap that will be introduced in Section 3.4. The offset surface is extended 5 mm and cuts the boundary plate (Figure 14C). The plate is finished by smoothing the edges and subtracting the screws and k-wires from the plate (Figure 14D).

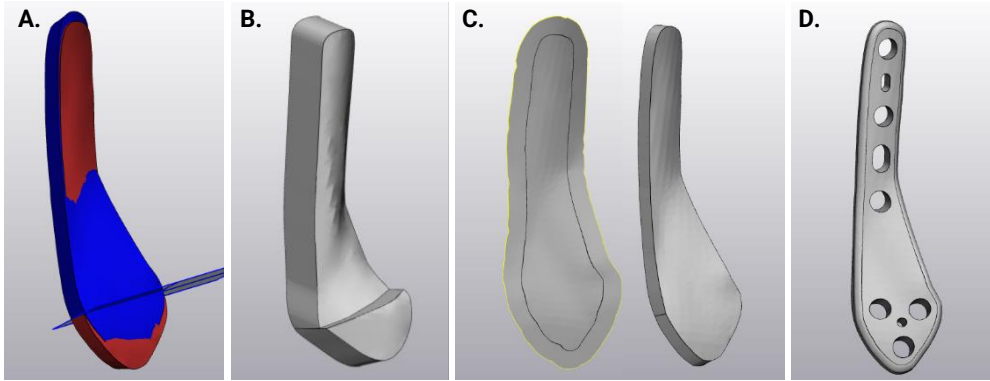


Figure 14. Give the plate thickness by a) creating boundaries for the proximal and distal part and b) a uniform offset for the required thickness and c) finish the plate.

3.4 Mechanical Safety

3.4.1 Introduction

Most design requirements of the patient-specific plate are derived from measurements in generic certified plates or prior literature, and therefore ensure mechanical safety. A patient-specific aspect that has not been addressed in literature or generic plates, is the varying longitudinal curve of the plate. The curve matches the femur of the patient and bridges the step resulting from the closed wedge osteotomy. The variability in plate shape due to individual anatomical differences could potentially result in a higher plate stress compared to a generic plate. While it is possible to estimate the bending behavior of a curved plate by comparing it to simple bending of a beam, as described in Appendix B, the exact effect of the curve on the stress cannot be predicted.

The objective of this study is to design the patient-specific plate to withstand the maximum load the generic plate can hold without yielding successfully, by determining the required thickness depending on the longitudinal curve of the plate. This objective is essential to meet the design requirement that the stress in the plate must be similar to, or smaller than, the stress in a generic plate under the same loading, ensuring the mechanical safety of the plate. The primary stress parameter is the von Mises stress, a measure of the combined effect of stress in three perpendicular directions. This stress can be compared to the material's yield strength to determine if failure is likely to occur. To determine the required thickness for varying curved plates so that it is sufficiently strong, an extensive simulation of the plate, screws and bones under physiologically relevant loads should be conducted in a finite element analysis (FEA). However, as a first approximation, the complexity of the model is reduced and a simplified method is used, and screws, bone, contact interactions, muscle forces and joint reaction forces are not considered.

3.4.2 Methods

Finite element models are constructed for the generic and patient-specific plates, allowing for application of loads and fixations directly on the screw holes. The first step is to determine the maximum load that the generic plate can hold without yielding, and then subject the patient-specific plate to the same load. Then, the thickness required to withstand that load successfully can be determined for varying longitudinal curves.

Plate models

Generic plate

The generic plate used to determine the maximum load is a Newclip, ActivMotionS, Medial Closing Distal Femur Osteotomy Plate. Newclip Technics produces osteosynthesis material since 2001. They received CE certification for all its products under the new medical device regulation (MDR) (EU 2017/745), and via the ISO 13485 standard. The plate was scanned with a laser scanner (E2, 3Shape, Copenhagen, Denmark) with an accuracy of 10 μm . Preprocessing was performed in Autodesk Fusion 360 (2020 Autodesk, Inc), reducing the STL with an adaptive mesh

with a factor of 0.1. The screw holes were simplified for analysis by closing the threaded screw holes and subtracting cylinders at the positions of the screws (Figure 15). The mesh was converted to a solid for further analysis.

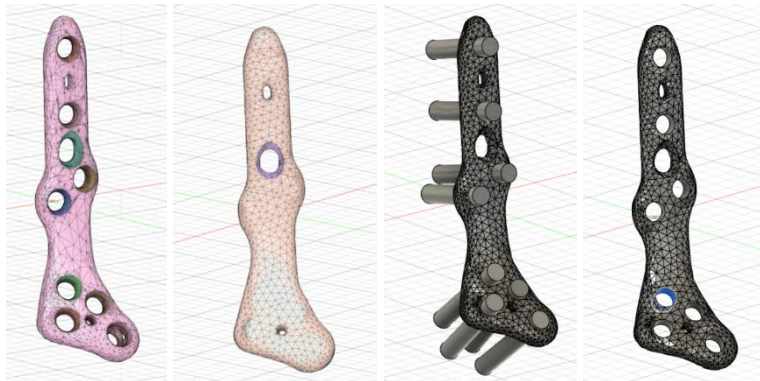


Figure 15: Preprocessing of the Newclip plate, reducing the mesh and simplifying the screw holes.

Patient-specific plate

A three-dimensional model of the patient-specific plate was designed, using computer-aided design (CAD) software (SOLIDWORKS 2022, Dassault Systems, Massachusetts, USA). The patient-specific osteotomy plate was designed according to the specifications for the basic shape described in section 4.2 *Statement of Requirements*. Exceptions were made for specifications based on individual patient anatomy, including the plate profile, in this research designed by simple curves. The longitudinal curve was defined by two variables: the offset and distal angle (Figure 16). The offset is the distance over the bridging span perpendicular to the proximal axis. The offset was varied between 3 and 21 mm. The distal angle is the angle between the axis along the proximal part and axis along the distal part of the plate. This angle ranged from 0 to 25 degrees. The range of both variables was based on the extreme measurements of the curve in the generic plate and of the curve in five patient-specific plates.

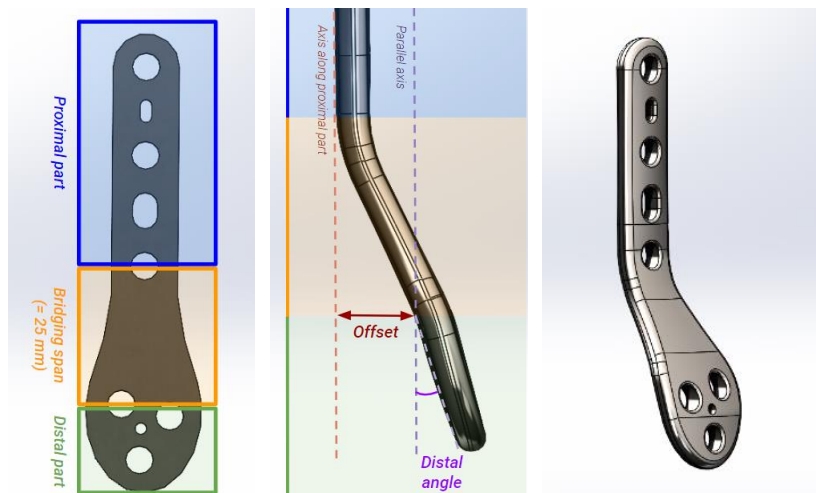


Figure 16: The definition of the offset and distal angle, serving as parameters that define the longitudinal curve of the patient-specific plate.

The properties of treated and aged Ti6Al4V incorporated in Solidworks were adopted into the simulated implant models. The Young's modulus was set at 104,800 MPa with a Poisson's ratio (ν) of 0.31⁶⁵. Both plates were modelled to incorporate linear elastic, isotropic, and homogeneous properties.

Finite Element Analysis

Determination of representative maximum sustainable load

To establish a mechanical safety similar to a generic plate, the maximum load before the generic plate yields was calculated in a FEA. Knowing that this plate is made out of a titanium alloy, mechanical properties similar to that of aged Ti6Al4V were assumed.

The maximum load for the Newclip plate before exceeding the yield strength was determined in a FEA as shown in Figure 17. The pre-processed model of the Newclip plate was meshed using a 0.4 – 3.0 mm blended curvature-based mesh. The proximal screw holes were fixed in all degrees of freedom to prevent rigid body motions during the analysis. An increasing axial force in steps of 100 N with an equal distribution over all distal screws was applied to simulate the axial compressive load through the screws. The direction of the axial force was along the second proximal screw to the upper proximal screw. The maximum load was defined as the highest load applied to the distal forces, without the maximum von Mises stress in the plate exceeding the yield strength of 827 MPa⁶⁵. The yield strength is a material property incorporated in Solidworks for treated and aged Ti6Al4V.

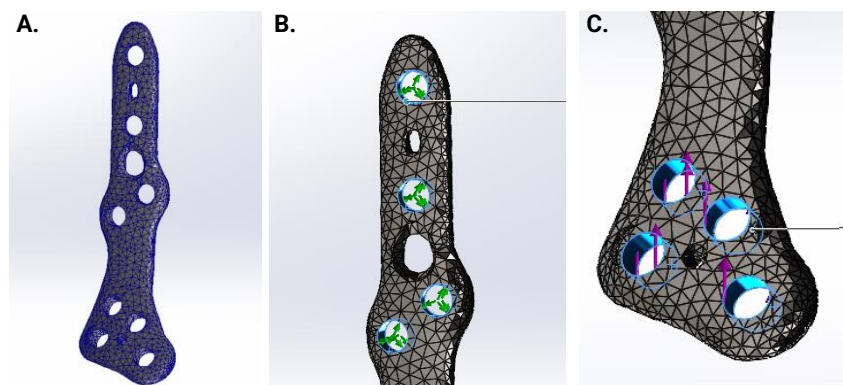


Figure 17: Finite element model of the Newclip plate, showing a) the mesh, b) the fixed proximal screw holes with green arrows, and c) the axial load on the distal screw holes with purple arrows.

Coarse grid calculation of the required thickness

The thickness required to resist the calculated maximum load was determined for 42 combinations of offset and distal angle. Respective ranges of offset and angle were 3 mm to 21 mm in steps of 3 mm, and 0° to 25° in steps of 5°. This was done in an iterative way. First, an analysis was performed with an estimated thickness t_{est} . The plate was meshed and the proximal screw holes were fixated. The maximum load was applied to the distal screw holes in direction

from the second proximal screw hole to the upper proximal screw hole, and the maximum occurring stress $\sigma_{est.max}$ was determined (Figure 18). Then, a new thickness t_{new} was determined, since in general the maximum stress is proportional to the squared thickness as derived in Equation:

$$\sigma_{b.max} \cdot t^2 = 827 \cdot t_{new}^2 \xrightarrow{\text{yields}} t_{new} = \sqrt{\sigma_{est.max} \cdot t_{est}^2 / 827} = \sqrt{\sigma_{est.max} / 827} \cdot t_{est}$$

The thickness of the plate was adjusted and the stress analysis was repeated. This process was repeated until the maximum von Mises stress measured was equal to the yield strength, with a margin of 10 MPa under the yield strength (8.17 – 8.27 MPa).

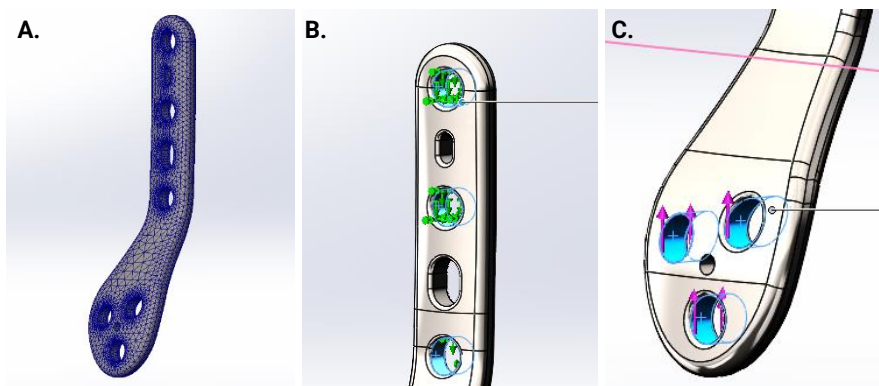


Figure 18: Finite element analysis of the patient-specific plate, showing a) the mesh, b) the fixed proximal screw holes with green arrows, and c) the axial load on the distal screw holes with purple arrows.

Fine grid calculation of the required thickness

The combinations of offset, distal angle and required thickness were imported in MATLAB (version R2019b, The MathWorks Inc.). The sample points were interpolated in steps of 1 mm for the offset and 1° for the distal angle, using cubic interpolation. The output was visualized in a 3D plot to examine the effect of the offset and distal angle on the required plate thickness. For clinical use of the model, the thickness measurements were rounded up to one decimal place and visualized in a heatmap.

3.4.3 Results

The FEA of the generic Newclip osteotomy plate resulted in a maximum von Mises stress of 806 MPa under a load of 3000 N. When the load was increased to 3100 N, the maximum stress in the plate was 833 MPa, exceeding the yield strength for titanium alloy of 827 MPa (Figure 19).

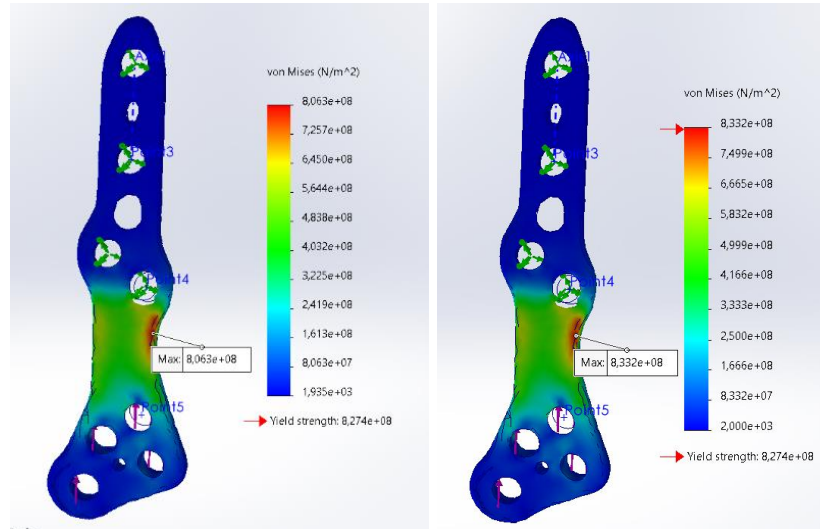


Figure 19: The von Mises stress in the Newclip plate under a load of a) 3000 N and b) 3100 N.

For varying curves of the patient-specific plate, the thickness required to hold a load of 3000 N is visualized in Figure 20.

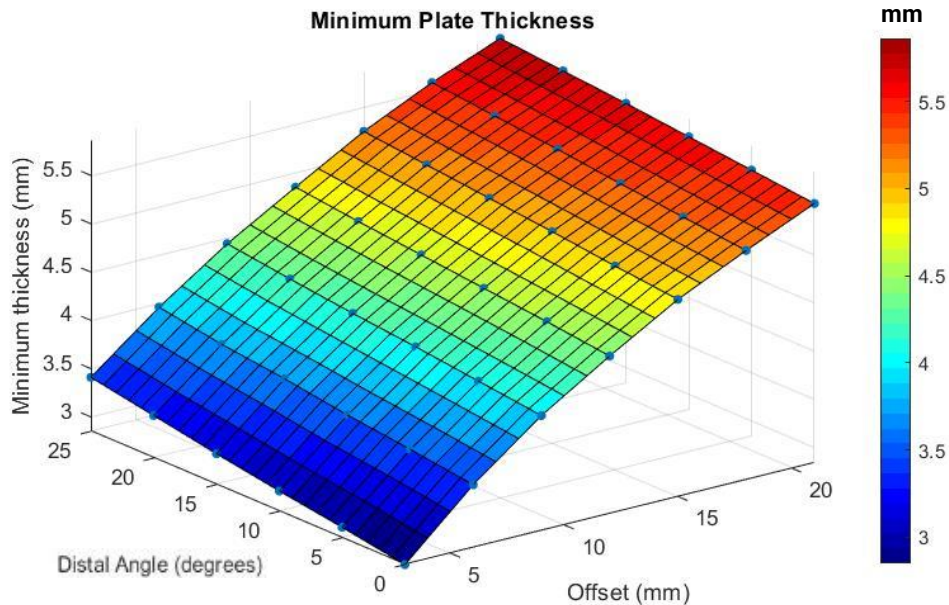


Figure 20: The minimum plate thickness in relation to the distal angle and the offset of a patient-specific plate to resist a load of 3000 N.

For clinical use of the model, the resulting values for required thickness depending on the offset and distal angle are rounded up to one decimal place and visualized in a heatmap, provided in Figure 21.

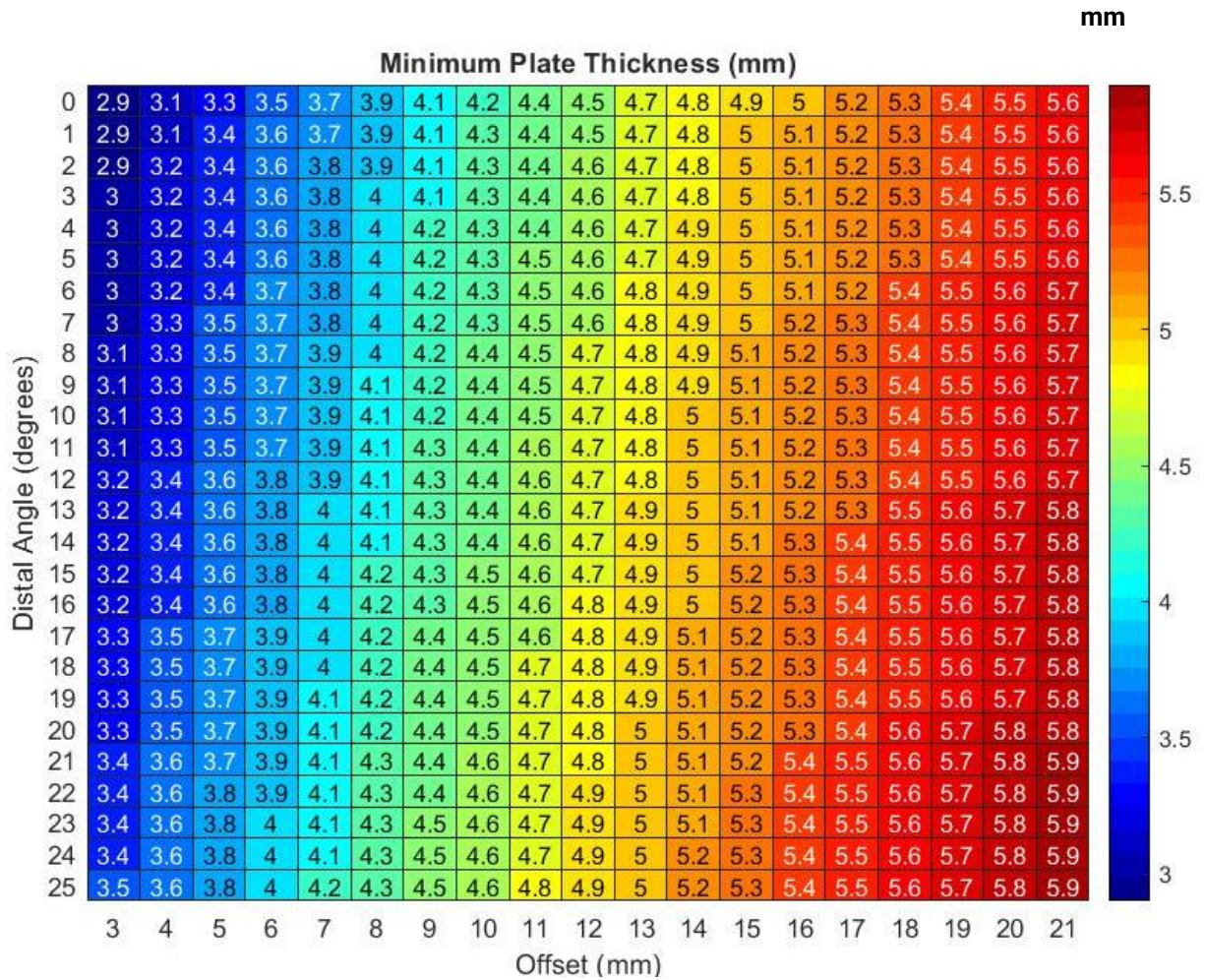


Figure 21: Heatmap visualizing the required thickness of a patient-specific plate to resist a load of 3000 N, depending on the offset and distal angle

3.5 Discussion: Design

In this chapter, design requirements and a design workflow have been proposed for the development of a patient-specific closed wedge DFO plate. An estimation was made of the required plate thickness in a Finite Element Analysis, to ensure mechanical safety.

Design specifications, requirements, and workflow

A strength of this design is that it can be applied to patients with various bone deformities, while no prior literature was found validating patient-specific plate design in this specific patient group. Additionally, the proposed workflow is tailored for use within the UMCU, allowing for direct clinical implementation.

A limitation concerns the inclusion criterium that a patient is eligible for a patient-specific plate when the maximum plate-bone distance is greater than 10 mm. In the absence of research investigating this correlation, the limit for the distance was estimated by orthopedic surgeons specialized in osteotomies, based on the distance on which soft tissue irritation is expected. Further research is required to determine the clinically relevant plate-bone distance, for example correlating the plate-bone distance measured on post-operative CT-scans with incidence of soft tissue irritation or plate removal.

Another limitation involves the potential impact of varying angles between the plate and screw orientations. This arises from two patient-specific design requirements. First, the distal screws are oriented towards the mechanical axis, and second, the shape of the plate is congruent with the patient's femur. While other patient-specific characteristics have been investigated in literature, generic certified plates or in the mechanical safety test, the effects of the plate-screw angle were not considered. Since locking screws are used in the patient-specific plate design, this should have no effect on the screw-plate interface. However, it might influence the forces or stress within the screw plate construction.

Mechanical safety

The aim of the mechanical safety study was to determine the required thickness of patient-specific plates with varying longitudinal curves, so that it does not yield under the maximum load that the certified Newclip plate can hold without yielding.

The maximum axial load for the Newclip plate before exceeding the yield strength was determined in a FEA. It is important to note that the maximum load primarily served the purpose of calibration between the Newclip model and the patient-specific model. In prior research, a maximal axial force of 3.1 times the body weight was measured during the gait cycle and up to 5.4 times the body weight during stair climbing⁶⁶. Additionally, in the UMCU patients with a DFO are advised to limit physical load on the knee to 50% and gradually increase it to 100%. The clinical guidelines may vary per type of osteotomy and per clinic, as research showed that early full weight-bearing after open wedge HTO without bone graft leads to earlier improvement of the

clinical results⁶⁷. The measured maximum load differs from prior research due to the assumptions made in the simplified model.

The relationship between the offset, distal angle and required thickness are visualized in a 3D plot and converted into a heatmap for clinical application. These relationships can be partially understood through the bending behaviour of a simple beam, as derived in Appendix B. The squared thickness of the plate is proportional to the bending moment. Therefore, a linear relationship is expected between the offset and the bending moment and a sinusoidal relationship for the distal angle, as the distance to the fixed screws increases when the parameters increase. However, in addition to the stress caused by the bending moment, the stress in the curved plate as measured in the FEA is also caused by compression. Therefore, the stress in the plate is more complex to predict, supporting the added value of the FEA.

The most important strength of the mechanical safety study is the usability of the study's findings in clinical practice. The generated heatmap offers immediate determination of the thickness for each possible curve of a patient-specific plate, without the need for further analysis or calculations for each individual plate. Another strength is the simplicity of the method used to evaluate mechanical safety. Assumptions based on literature and design characteristics of certified generic plates, allowed for a simplified FEA. This approach eliminates the need for extensive expertise, computing power, and computing time that are typically required for assessing the mechanical safety of a personalized plate⁴⁵.

The assumptions and simplifications made in this study introduce three key limitations. The first limitation is that the forces applied to the plate may not accurately represent the forces on a plate in a patient. The load on the plate is simplified by simulating an axial force directly on the distal screw holes and fixating the proximal screw holes. In a closed wedge osteotomy, axial load is not only transferred by the screws, but also carried by bone-to-bone contact and by the hinge. A more extensive model, including screws, bone, contact interactions, muscle forces, and joint reaction forces, might provide a more realistic representation of the complex biomechanical behavior and loading conditions that occur in a clinical setting.

A second limitation is that the von Mises stress is the only outcome measures considered to determine the required thickness. Although the increased thickness reduces von Mises stress within the plate, the increased rigidity could induce stress shielding and restrict IFM. IFM is essential for callus formation, and a lack of bone consolidation over the long term increases the risk of fatigue failure of the plate³⁹. To measure the IFM, it would be necessary to include both the screws and bone in the FEA.

A third limitation is that the standardized curved plates analyzed in this study may not be representative of the more complex shaped patient-specific plates that are designed for clinical practice. The shape of the patient-specific plates is not only based on the longitudinal curve, but constructed with an additional 3D outline that corresponds to the individual's femur. Furthermore,

the longitudinal curve in the FEA is only defined by the offset and distal angle, whereas the longitudinal curve in the patient-specific design is a more complex spline. Adding more parameters to approach the shape of the plate more closely would result in more accurate measurements of the stress in the plate. However, it requires more time and makes the analysis and clinical use more complex. Therefore, a standardized outline was used and only two parameters were selected to define the longitudinal curve, based on preliminary tests determining which parameters had the most effect on the stress in the plate, including parameters offset, distal angle and maximum angle. Further research is required to confirm that the standardized plates used in this analysis are representative for the patient-specific plates.

Future research to address these limitations and to validate the mechanical, would involve an extensive and personalized FEA, incorporating a patient-specific plate, bone model and loading conditions at different healing stages. A similar study was conducted by MacLeod et al. (2021)⁴⁵ in a case-control in-silico virtual clinical trial. They compared the mechanical safety of a personalized 3D printed osteotomy device designed to match individual tibia geometry to an existing generic device. A FEA was performed to calculate the maximum von Mises stress within the plates, the maximum Von Mises strain in the bone adjacent to the screws and the IFM at the osteotomy site. Three physiological activities were simulated, including fast walking gait, chair rise, and squat. Osteotomy gap bone healing was simulated by increasing the Young's modulus of the material in the gap for different healing stages. The in-silico trial showed that there is no increased risk of failure and no difference in stability indicated by IFM. However, the authors highlighted significant challenges, such as the considerable user input required to produce subject specific models, and the computing time of more than half a million core hours to produce solutions of the models. It should be considered that developing a virtual clinical model is comprehensive and complex.

4 Validation

4.1 Validation Design Workflow

Introduction

To design a patient-specific closed wedge DFO plate, a statement of requirements and a workflow that meets the requirements have been provided in previous chapter. In this section, the design workflow is conducted and a check is done to see if the resulting patient-specific plates met the design requirements for a wider sample within the patient group. Furthermore, the variety in the longitudinal curves of patient-specific plates is explored to check if the resulting required thickness is feasible. Therefore, a case study is conducted to validate the design workflow and to explore the shape and required thickness of the plates.

Method

Patients

Patients with bone deformities were included who are treated or scheduled for closed wedge DFO in the University Medical Center Utrecht, according to the current 3D workflow for complex patients. Inclusion criteria were similar to the intended patient group described in Section 3.1.

Protocol

Pre-operative planning was conducted as described in the clinical workflow in Section 3.1 (Figure 22), using the Newclip ActivMotionS closed wedge DFO plate for fixation (Newclip Technics, Haute-Goulaine, France). Patient-specific plates were designed according to the guidelines outlined in 3.3 *Design Workflow*.



Figure 22: The design workflow tested in this case study is colored in blue and orange. Remaining steps of the full clinical workflow that are not considered in this validation are colored gray.

Measurements

Measurements were conducted in the resulting patient-specific plates to check if the design requirements described in Section 3.2 were met. The plate-bone gap and the plate-bone distance were measured in the software Materialise, using the part comparison function. The plate-bone gap was defined as the distance between the cortex and the inner side of the plate. The plate-bone distance was the distance between the cortex and the outer side of the plate, including the thickness of the plate. All other design requirements regarding screw position and shape of the plate were automatically met if the design workflow can be carried out according to protocol, and therefore required no measurements. The offset and distal angle of the longitudinal curve of the plate are measured as described in Section 3.3 under *adaptation to parameterized shape*, and shown in Figure 13C. Based on the curve, the required thickness of the plate was derived from the heatmap shown in Figure 21.

Results

A total of five patients were included. Patients' characteristics, the planned location, and correction of the osteotomy are provided in Table 2.

Table 2: Patient characteristics

Patient	Sex (F/M)	Age (years)	Length (mm)	Weight (kg)	DFO location (left/right, medial/lateral)	Correction (degrees, direction)	Cause deformity
1	M	22	169	68	Left, lateral	8, sagittal	Hypofosfatemic rachitis
2	F	54	153	72	Right, medial	11, sagittal	MED
3	F	28	155	70	Right, medial	6, sagittal	Femur Fibula Ulnaris Syndrome
4	F	43	152	56	Right, medial	17, sagittal	CODAS syndrome
5	F	23	128	53	Right, lateral	10, sagittal	Achondroplasia

For all five patients, the design workflow was conducted, a patient-specific plate is designed, and the plate-bone gap of the patient-specific plate was measured. Measurements of the plate-bone distance for both plates and of the curve of the patient-specific plate are provided in Table 3.

Table 3: Measurements of the plate-bone distance

Patient	Max plate-bone distance Newclip plate (mm)	Max plate-bone distance novel plate (mm)	Max plate-bone gap novel plate (mm)	Offset longitudinal curve novel plate (mm)	Distal angle longitudinal curve novel plate (degrees)	Required plate thickness (mm)
1	11.5	7.9	3.4	10	10	4.4
2	10.8	7.2	1.9	11	25	4.8
3	11.4	7.2	1.8	16	7	5.2
4	13.2	6.5	0.8	18	4	5.3
5	10.0	5.5	0.4	7	14	4.0

Visualizations of the plate fittings and plate-bone distances are added in Appendix C, with an example shown in Figure 23. The plate-bone distance is quantified in millimeters and represented in Figure 23C and D, using a color-coded scale.

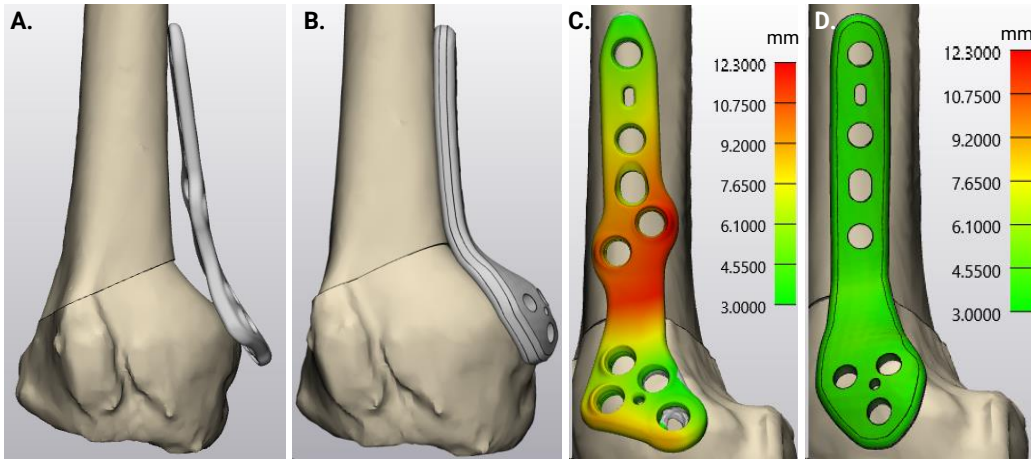


Figure 23: A virtual osteotomy is conducted for a) the Newclip plate and b) the patient-specific plate. The plate-bone distance is quantified in millimeters and represented using a color-coded scale for c) the Newclip plate and d) the patient-specific plate.

The plate-bone gap for all plates are visualized in Figure 24. The color-coded scale represents the plate-bone gap in mm. The minimum values in the color bars are negative due to plate-bone overlap. The maximum value in the color bar is limited to 2 mm added to the minimum value. A plate-bone gap that exceeds the limit of 2 mm in colored in grey. For two out of five plates, the maximum plate-bone gap is less than 2 mm over the entire plate. For two plates the distance exceeds the limit of 2 mm at the height of the bridging span, but the proximal and distal parts are within the 2 mm distance. The plate for patient 2 exhibits a distance greater than 2 mm in the proximal part, failing to meet the design requirement.

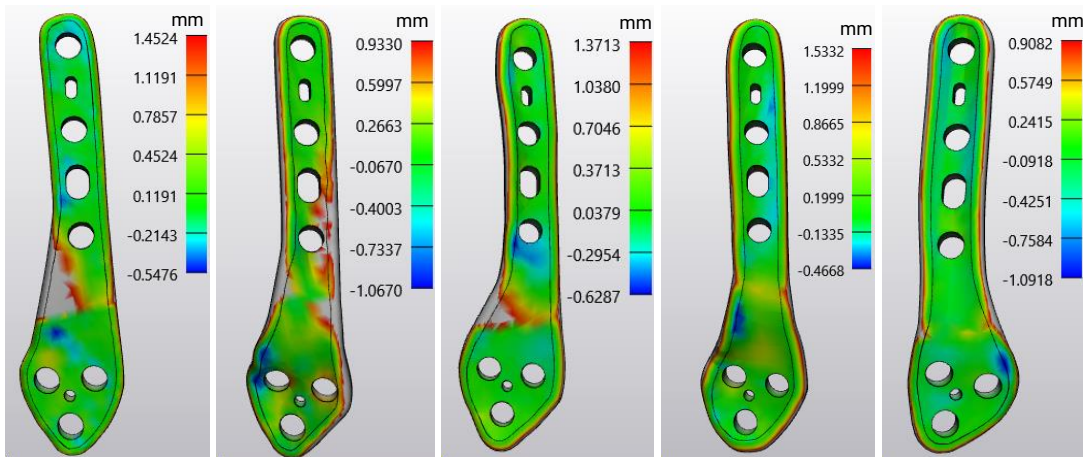


Figure 24: The plate-bone gaps are visualized for all patients, with scales ranging from the minimum distance to a 2 mm addition beyond the minimum.

4.2 Manufacturing and Costs

Manufacturing

Manufacturing the plate, whether through 3D printing or milling, involves several key steps, including file preparation, machining, heat treatment, screw hole milling, polishing, and sterilization (Figure 25). File preparation is performed by the 3D specialist responsible for the plate design, and is therefore further elaborated upon. The type of manufacturing, namely 3D printing or milling, has a significant impact on the plate's properties and design. Therefore, this consideration is also described. The manufacturing process is outsourced to an external manufacturer, specialized in medical instruments and equipment. A wide range of manufacturing techniques, heat treatments and polishing are available. Details on the machining and finishing process highly depend on the techniques out of the wide range of manufacturing techniques, therefore left outside the scope of this thesis. Important to note, is that the legal manufacturer of the patient-specific plate is the department Medical Technology and Clinical Physics within the UMCU. The internal quality safety system according to ISO 13485, allows for safe and legal *in-house* design of medical devices, while outsourcing the manufacturing process. Standard documentation, a certificate of conformity and a material certificate for traceability are provided by the manufacturer.



Figure 25: The workflow for manufacturing the patient-specific plate colored in orange, described within the full clinical workflow colored in gray.

File preparation

The file type required for manufacturing depends on the manufacturing technique. If the plate is 3D printed, the plate can be exported as an STL-file directly from the Materialise software. If the plate is milled, a STEP-file is required to plan the milling path. The plate design in Materialise is too complex to export directly as a STEP-file, as the format is interoperable among software used for toolpath generation for milling. Therefore, the file is converted in Autodesk Fusion 360 (2020 Autodesk, Inc). The base plate with straight edges and without screw holes, and the screws are exported from Materialise as an STL-file. The plate and screws are uploaded in Autodesk and converted to a solid. The edges of the plate are smoothed using the fillet option and the screws are subtracted from the plate. The result can be exported as a STEP-file.

Printing or milling

The patient-specific Ti6Al4V osteotomy plate can be either 3D printed or milled. 3D printing allows for complex geometries, can be cost-effective for small-scale production due to its flexibility and reduced material waste, and allows for rapid prototyping and productions as milling involves multiple steps and longer lead times⁶⁸. However, the shape of the plate is based on simple curves and time is not a constraint. Moreover, the plate requires precise mechanical properties such as strength and durability to ensure mechanical safety. Milling is less likely to introduce variability in the material compared to 3D printing. Also, milling techniques can provide excellent surface finish

and dimensional accuracy, potentially reducing or eliminating the need for additional post-processing steps.⁶⁹ Therefore, milling is preferable to 3D printing.

Milling titanium poses several machining challenges. First, the high chemical reactivity causes titanium to weld to the tool. Second, the low thermal conductivity increases the temperature at the tool-plate interface. Third, the low elastic modulus of titanium causes the material to spring away from the cutting tool, increasing friction and raising the temperature.⁷⁰ Additionally, a practical challenge of milling involves the clamping technique. Either the plate must be placed within a mould or the path has to be programmed to preserve three points of contact that are removed during the final stage. Testing of the setup and selection of proper metalworking fluid are essential to improve the surface characteristics and integrity⁶⁹.

Costs

There are various costs component additional to the costs of the current workflow for patients with bone malformations using a generic plate and a PSI. Additional costs during the *design phase* arise mostly from labor costs, including those of the 3D expert, the orthopedist and the MTCP expert. The 3D expert makes the initial design (estimated around 3 hours), all three evaluate the design (0.5h), the 3D expert makes design adjustments (1h), and the 3D and MTCP experts invest time in documentation and certification of the plate design. The required software is available within the UMCU and will not incur extra costs. To facilitate training, expenses will be incurred for the 3D expert to become familiar with the design workflow (2h). To test the workflow and to familiarize the orthopedics with the patient-specific plate, a test osteotomy will be conducted, entailing working hours (1h) and printing costs for a 3D printed bone out of polylactic acid, and a PSI and plate out of polyamide-12.

The most significant costs of the *manufacturing process* include 1) the costs for the titanium alloy used in the plate, 2) the machinery and software necessary for file preparation, printing/milling, heat treatment, screw hole tapping, polishing, sterilization, documentation, and certification, 3) labor costs of the manufacturer, and 4) the expertise required to address machining challenges and test the setup. Manufacturing can be outsourced to the regional ISO 13485 certified medical company, Witec (Witec Medical B.V., Stadskanaal, the Netherlands). They use a 5-axis milling machine to make a plate of medical grade titanium alloy by computer numerical control milling. The costs for the first plate are estimated around 3700 euro, which might decreased when plates are produced on a monthly basis. The costs for a generic plate are estimated around 700 euro. The patient-specific plate requires two titanium alloy locking screw less, which are estimated around 80 euro per screw.

Potential costs savings could be realized when a second operation for plate removal would be avoided and when the operating time would be reduced. However, reduced operation time is not expected in the first cases. To conclude, it can be assumed that the patient-specific plate involves greater expenses compared to the generic plate. A more detailed cost-benefit analysis could be conducted to determine whether the benefits outweigh the additional costs.

4.3 Risk Analysis

There are risks associated with the use of an *in house* developed patient-specific plate. Potential modes of failure during the design phase, manufacturing, per-operative, and post-operative phases can be identified. These failures may impact the accuracy of the correction and, in severe cases, may cause permanent injury to the patient. In this section, potential modes of failure and their consequences are described for each phase. A complete risk analysis corresponding measures for each potential mode of failure is provided in Appendix D.

Table 4: Potential modes of failure associated with the patient-specific plate.

Potential mode of failure	Consequence	Severity
Design		
The product is designed in such a way that cleaning and sterilization are not straightforward, leaving residue	Plate might be unsterile or residue is left in the patient	Permanent injury
The plate is designed in a way that it cannot be properly placed on the femur or screws cannot be placed	Operation must proceed with a generic plate	Reversible injury
The plate design does not align with the pre-drilled screw holes guided by the PSI	Extra screw holes need to be drilled, or the operation must proceed with a generic plate and accuracy of the correction is not ensured	Reversible injury
The plate is not applicable as intended by the physician (poor communication between 3D lab and physician)	Operation must proceed with a generic plate	No injury
Manufacturing		
An error occurs during finishing	Biocompatible properties and mechanical safety are not ensured	Permanent injury
The plate is damaged during finishing	Operation must be postponed or must proceed with a generic plate	No injury
Usage		
The plate is not available on time	Operation must be postponed or must proceed with a generic plate	No injury
The plate is found not to fit well on the femur during the operation	Operation must proceed with a generic plate	Reversible injury
Facilities (ICT/sterilization)		
Incorrect sterilization method is applied to the plate	Damage or deformation of the plate	Permanent injury
Software malfunctions or crashes	The plate cannot be designed according to the design workflow, or not at all	No injury
An outdated version of the CAD/CAM software is used	Possible new improved functionalities are not implemented	No injury
Lifecycle		
The implant cannot be removed when necessary	Surrounding bone structure must be removed along with the implant during removal	Permanent injury
The plate experiences mechanical failure	The plate must be removed and replaced if the bone parts are not consolidated	Reversible injury

Risk-reducing measures

Several measures are taken to reduce the risk of failure. During the design phase, the design is checked for angles that cannot be cleaned or sterilized. The surgeon and 3D specialist discuss the virtual osteotomy, PSI and plate design in a meeting prior to the surgery to align expectations and intentions of the correction and design. Additionally, the surgeon's signature is required for the order file to gain early insight into the design. Then, the surgery is practiced on a nylon 3D printed bone model, PSI and plate, thereby minimizing the risk of design errors and operational mistakes. The titanium plate is manufactured by an external ISO 13485 certified medical company, and their protocol is followed to prevent failures during manufacturing. In case the operation must proceed with a generic plate, the surgeons are trained to perform the surgery according to the current protocol. However, the deformity of the bone might complicate the fixation and because the pre-drilled screw holes cannot be used for plate positioning, the accuracy of the correction is not ensured. The most significant associated risk is mechanical failure of the plate. This risk is reduced by adjusting the thickness of the plate to the stress, as explained in Section 3.4. Clinical follow-up is performed in iProve at standardized moments in time. The patient will be informed of the risks prior to the entire design process in an informed consent meeting.

4.4 Discussion: Validation

In this chapter, a validation has been performed for the patient-specific plate design, including a virtual validation of the design workflow in five patients, and exploration of manufacturing, costs, and risks.

Validation design workflow

The workflow was successfully executed for all patients, meeting most requirements for screw positions and shape of the plate. For 4 out of 5 patients, the plate-bone gap fell within a range of 2.0 mm, which satisfies the design requirement. However, for one patient, the plate-bone gap extended up to 3.4 mm. The distance could be decreased, adding more curves as guiding lines when constructing the surface of the base plate. However, it should be considered that this results in a more complex curve, which can influence the forces and stress in the plate and screws. The optimal balance between fitting the plate to the bone and the complexity of the shape of the plate is yet to be determined.

The longitudinal curve of the plate extended to a maximum offset of 18 mm and a maximum distal angle of 25 degrees. Based on the estimation of the required thickness made in Section 3.4, the plates designed in this section had thicknesses ranging from 4.0 to 5.3 mm. This did not pose difficulties in the design workflow. The maximum plate-bone distance was still reduced from 9.6-12.3 mm for the generic plate to 5.5-7.9 mm for the patient-specific plate, despite the increased thickness. In all cases, the maximum distance was less than 10 mm, which is hypothesized to cause less soft tissue irritation. However, the effects of the increased thickness, such as stress shielding, need to be further investigated alongside the von Mises stress in the plate.

A limitation is that *Patient 2* was included both in the validation data and used for improving the design workflow, introducing a bias in the validation results. It is worth noting that this patient did not show better results compared to other patients, and considering the exploratory nature of this study, the bias may not be relevant.

Future research could involve implementing the virtually validated design into clinical practice. It is important to note, that soft tissue and inaccuracy of the correction were not considered in the virtual validation. Ligament laxity and soft tissue contractures in patients in bone deformities might complicate the surgical procedure²⁹. As the surgical approach, osteotomy, use of PSI, and fixation with a plate are similar to the current clinical workflow, no additional intraoperative complications or logistical issues are expected. However, the accuracy of the osteotomy achieved in practice may deviate from the virtual designs. A systematic review investigating the accuracy in osteotomies using a PSI, reported a mean error of 0.8° HKA angle and 0.6° for the posterior tibial slope³¹. Additionally, the plate-bone distance might be increased by periosteum on the bone surface, which is not visible on the CT scan. Consequently, achieving a plate-bone gap smaller than 2 mm might not be feasible in practice, and the actual plate-bone distances are expected to be greater than those measured in the virtual validation.

Manufacturing and costs

Based on the exploration of the manufacturing process, milling was considered more preferable compared to 3D-printing. While challenges associated with the milling process were identified, it is not anticipated to pose a significant problem, as the feasibility of this manufacturing method was demonstrated by the 3D lab in Groningen⁴⁴. The cost difference is primarily due the manufacturing process, with an estimated additional cost of 3000 euros, and increased labor costs during the design phase. A more detailed cost-benefit analysis could be conducted to determine whether the benefits outweigh the additional costs.

A limitation of the exploration of the manufacturing process is that it has been examined independently of the clinical workflow, while the manufacturing technique may influence certain design choices, and vice versa. For instance, a generic proximal part of the plate could be placed in a mould for clamping during milling. Milling using the three-point clamping technique would not require design adjustments. Another example could be that certain angles are too complex for milling. None of the five plates designed so far have included such angles. Required design adjustments can be identified once the manufacturing process is refined in collaboration with the manufacturer.

Risk analysis

Significant risk-increasing modes of failure include design flaws that complicate plate removal or increase the risk of mechanical failure, and flaws in the manufacturing and sterilization process, which could result in permanent injury. Therefore, risk-reducing measures associated with these processes are strongly advised. For other risk-reducing measures, especially the practice osteotomy on a 3D printed bone model, PSI and plate, a cost-benefit evaluation may be worth considering.

A limitation of the risk analysis is that the scoring system rates the risk as low, driven by the estimation that the likelihood of failure is less than once a year. However, this estimation is based on the idea that approximately one plate is developed per month. It might be informative to assess the risk on a per-patient basis to gain a more accurate understanding of the risk profile.

5 General Discussion

In patients with rare bone deformities, the abnormal geometry of the bone and altered biomechanics raise some technical challenges when it comes to fixation with a generic plate after an osteotomy. Patients suffer from soft tissue irritation, procedures have longer operation times, and mechanical safety may not be assured. This study aimed to develop a workflow for *in-house* design of a patient-specific plate in malalignment surgery with 3D technology, achieving mechanical safety comparable to that of a generic certified plate, in patients for whom *off the shelf* solutions do not fit. The mechanical safety, feasibility, and future perspective are discussed in this section.

This study aimed to ensure mechanical safety by thoroughly establishment of individual design requirements that influence mechanical safety, based on literature, measurements in generic plates, or estimations derived from a simplified FEA. However, it is essential to consider that the plate's shape, strength, manufacturing process and their interplay with the screws and bone are closely interrelated and affect each other.

Future research could be considered for a validation of the mechanical safety. This could involve an extensive and personalized FEA, incorporating the patient-specific plate, bone model and loading conditions at different healing stages. However, the development of such a model requires extensive expertise, computing power, and computing time⁴⁵, and there remains uncertainty regarding whether the model accurately represent clinical practice. Especially given the diverse biomechanics among the patient population, standard load models may not be applicable. An alternative to FEA could involve a tensile test, conducting the osteotomy with a milled patient-specific plate on artificial bones simulating bone architecture and physical properties. This approach would involve measuring static strength, IFM, and fatigue failure. However, this approach is considered unfeasible in clinical practice due to time constraints, high costs and the need for expertise. Given the complexity involved in further validation studies and the limited resources available for *in-house* development, the simplified and established approach applied in this study is considered adequate for ensuring mechanical safety.

Four key aspects described in this study contribute to the assessment of feasibility. Firstly, a competitive product analysis was conducted, identifying an alternative patient-specific fixation device named TOKA, developed by Orthoscape. While the MDR prohibits *in-house* production when a commercial alternative is available, since TOKA is focused on tibial plates and currently not available on the market, the relevance of *in-house* development remains intact. Secondly, the virtual validation indicated that the designed plates generally meet the requirements. However, an exception was observed in the plate-bone gap for one out of five patients. Further research is recommended to determine the optimal balance between plate-bone fitting and complexity of the plate shape. Thirdly, the cost analysis revealed that the patient-specific plates entail higher expenses compared to the generic plate. The cost difference is primarily due the manufacturing process, with an estimated additional cost of 3000 euros, and increased labor costs during the

design phase. A more detailed cost-benefit analysis could provide insights whether the benefits outweigh these additional costs. Lastly, the remaining risk associated with the use of a patient-specific plate is acceptable when suggested risk-reducing measures are implemented.

Several regulatory steps should be considered when the design is used for patient care. The proposed design workflow and presented research aligns with the well designed and successfully implemented framework employed by the UMCU for managing logistical and regulatory aspects of technology development⁴¹. This report serves as a technical file required for the development of a patient-specific medical device, in compliance with the quality management system. In the next phase, it is essential to collaborate with the MTCP as the legal manufacturer and the external manufacturer. With the involvement of all stakeholders, the manufacturing process can be further refined, and the remaining necessary documentation can be prepared.

Taken these aspects into consideration, *in-house* development of a patient-specific osteotomy plate demonstrates adequate mechanical safety and could be feasible when the benefits outweigh the costs. This is particularly promising for patients for whom a precise plate-bone fitting is crucial, and for patients with contraindications for a secondary surgical procedure for plate removal due to soft tissue irritation. The option of osteotomy for these patients is relevant, as it offers individuals with rare bone deformities the potential benefits of pain relief, improved mobility, postural correction, and the prevention of further complications such as premature development of OA²⁹. The decision to develop and apply a patient-specific plate should always be made collaboratively among the patient, physician and 3D specialist.

6 General Conclusion

In this study, a workflow has been successfully developed for *in-house* design of a patient-specific fixation device in malalignment surgery with 3D technology in patients for whom *off the shelf* solutions do not fit. To ensure mechanical safety similar to a generic plate, design requirements were based on literature, measurements in generic plates, and an estimation of the required plate thickness using a FEA. The virtual validation demonstrated that the design requirements were met for 4 out of 5 patients. For one patient, the 2 mm limit for the plate-bone gap was exceeded. Milling the plate was considered preferable. The patient-specific involves high additional manufacturing costs and increased labour costs during the design phase. *In-house* development could be feasible when the benefits outweigh the costs. Further research is recommended to conduct a more comprehensive cost-benefit analysis, and to determine the optimal balance between plate-bone fitting and the complexity of the plate shape.

7 References

1. Niet-traumatische knieklachten | NHG-Richtlijnen. <https://richtlijnen.nhg.org/standaarden/niet-traumatische-knieklachten#volledige-tekst>. Accessed October 20, 2022.
2. Primorac D, Molnar V, Rod E, et al. Knee Osteoarthritis: A Review of Pathogenesis and State-Of-The-Art Non-Operative Therapeutic Considerations. *Genes (Basel)*. 2020;11(8):1-35. doi:10.3390/GENES11080854
3. Heidari B. Knee osteoarthritis prevalence, risk factors, pathogenesis and features: Part I. *Casp J Intern Med*. 2011;2(2):205. /pmc/articles/PMC3766936/. Accessed June 21, 2023.
4. Mobasheri A, Van Spil WE, Budd E, et al. Molecular taxonomy of osteoarthritis for patient stratification, disease management and drug development: biochemical markers associated with emerging clinical phenotypes and molecular endotypes. *Curr Opin Rheumatol*. 2019;31(1):80-89. doi:10.1097/BOR.0000000000000567
5. Dell'Isola A, Allan R, Smith SL, Marreiros SSP, Steultjens M. Identification of clinical phenotypes in knee osteoarthritis: a systematic review of the literature. *BMC Musculoskelet Disord*. 2016;17(1):1-12. doi:10.1186/S12891-016-1286-2
6. Luís NM, Varatojo R. Radiological assessment of lower limb alignment. *EFORT Open Rev*. 2021;6(6):487. doi:10.1302/2058-5241.6.210015
7. Cooke D, Scudamore A, Li J, Wyss U, Bryan T, Costigan P. Axial lower-limb alignment: comparison of knee geometry in normal volunteers and osteoarthritis patients. *Osteoarthr Cartil*. 1997;5(1):39-47. doi:10.1016/S1063-4584(97)80030-1
8. Bellemans J, Colyn W, Vandenneucker H, Victor J. The Chitranjan Ranawat Award: Is Neutral Mechanical Alignment Normal for All Patients?: The Concept of Constitutional Varus. *Clin Orthop Relat Res*. 2012;470(1):45. doi:10.1007/S11999-011-1936-5
9. Felson DT, Niu J, Gross KD, et al. Valgus malalignment is a risk factor for lateral knee osteoarthritis incidence and progression: Findings from the multicenter osteoarthritis study and the osteoarthritis initiative. *Arthritis Rheum*. 2013;65(2):355-362. doi:10.1002/ART.37726
10. Brouwer GM, Van Tol AW, Bergink AP, et al. Association between valgus and varus alignment and the development and progression of radiographic osteoarthritis of the knee. *Arthritis Rheum*. 2007;56(4):1204-1211. doi:10.1002/ART.22515
11. Schröter S, Elson DW, Ateschrang A, et al. Lower Limb Deformity Analysis and the Planning of an Osteotomy. *J Knee Surg*. 2017;30(5):393-408. doi:10.1055/S-0037-1603503/ID/JR17MAR0006SSA-57
12. Farinelli L, Baldini M, Bucci A, Ulisse S, Carle F, Gigante A. Axial and rotational alignment of lower limb in a Caucasian aged non-arthritic cohort. *Eur J Orthop Surg Traumatol*. 2021;31(3):221-228. doi:10.1007/s00590-020-02763-7
13. Scorcelletti M, Reeves ND, Rittweger J, Ireland A. Femoral anteversion: significance and measurement. *J Anat*. 2020;237(5):811-826. doi:10.1111/JOA.13249
14. Song G-Y, Ni Q-K, Zheng T, Zhang Z-J, Feng H, Zhang H. Slope-Reducing Tibial Osteotomy Combined With Primary Anterior Cruciate Ligament Reconstruction Produces Improved Knee Stability in Patients With Steep Posterior Tibial Slope, Excessive Anterior Tibial Subluxation in Extension, and Chronic Meniscal Post. *Am J Sports Med*. 2020;48(14):3486-3494. doi:10.1177/0363546520963083
15. Lerch TD, Liechti EF, Todorski IAS, et al. Prevalence of combined abnormalities of tibial and femoral torsion in patients with symptomatic hip dysplasia and femoroacetabular impingement. *Bone Joint J*. 2020;102-B(12):1636-1645. doi:10.1302/0301-620X.102B12.BJJ-2020-0460.R1
16. Lim WB, Al-Dadah O. Conservative treatment of knee osteoarthritis: A review of the literature. *World J Orthop*. 2022;13(3):212. doi:10.5312/WJO.V13.I3.212
17. Gunaratne R, Pratt DN, Banda J, Fick DP, Khan RJK, Robertson BW. Patient Dissatisfaction Following Total Knee Arthroplasty: A Systematic Review of the Literature. *J Arthroplasty*. 2017;32(12):3854-3860. doi:10.1016/J.ARTH.2017.07.021
18. Noble PC, Conditt MA, Cook KF, Mathis KB. The John Insall Award: Patient expectations affect satisfaction with total knee arthroplasty. *Clin Orthop Relat Res*. 2006;452:35-43. doi:10.1097/01.BLO.0000238825.63648.1E
19. Elson DW, Petheram TG, Dawson MJ. High reliability in digital planning of medial opening wedge high tibial osteotomy, using Miniaci's method. *Knee Surgery, Sport Traumatol Arthrosc*. 2015;23(7):2041-2048. doi:10.1007/S00167-014-2920-X/TABLES/1
20. Driban JB, Stout AC, Duryea J, et al. Coronal tibial slope is associated with accelerated knee osteoarthritis: Data from the Osteoarthritis Initiative. *BMC Musculoskelet Disord*. 2016;17(1):1-7. doi:10.1186/S12891-016-1158-9/TABLES/2
21. Babis GC, An KN, Chao EYS, Rand JA, Sim FH. Double level osteotomy of the knee: a method to retain joint-line obliquity. Clinical results. *J Bone Joint Surg Am*. 2002;84(8):1380-1388. doi:10.2106/00004623-200208000-00013
22. Sherman SL, Thompson SF, Clohisy JCF. Distal Femoral Varus Osteotomy for the Management of Valgus

- Deformity of the Knee. *J Am Acad Orthop Surg*. 2018;26(9):313-324. doi:10.5435/JAAOS-D-16-00179
23. Bernhardson AS. Sagittal Plane Corrective Osteotomy Techniques. *Oper Tech Sports Med*. 2022;30(3):150932. doi:10.1016/J.OTSM.2022.150932
 24. Mattei L, Lea S, Nicolaci G, Ferrero G, Marmotti A, Castoldi F. 4 Basic principles of osteotomies around the knee. *Osteotomies around Knee*. 2013. doi:10.1055/b-0034-9884
 25. Zsidai B, Özbek EA, Engler ID, et al. Slope-Reducing High Tibial Osteotomy and Over-The-Top Anterior Cruciate Ligament Reconstruction With Achilles Tendon Allograft in Multiple Failed Anterior Cruciate Ligament Reconstruction. *Arthrosc Tech*. 2022;11(11):e2021-e2028. doi:10.1016/j.eats.2022.07.019
 26. Inan M, Ferri-de Baros F, Chan G, Dabney K, Miller F. Correction of rotational deformity of the tibia in cerebral palsy by percutaneous supramalleolar osteotomy. *J Bone Jt Surg Br Vol*. 2005;87-B(10):1411-1415. doi:10.1302/0301-620X.87B10.16712
 27. Raggio CL, Yonko EA, Khan SI, et al. Joint Replacements in Individuals With Skeletal Dysplasias: One Institution's Experience and Response to Operative Complications. *J Arthroplasty*. 2020;35(8):1993-2001. doi:10.1016/j.arth.2020.04.007
 28. Kim RH, Scuderi GR, Dennis DA, Nakano SW. Technical challenges of total knee arthroplasty in skeletal dysplasia. *Clin Orthop Relat Res*. 2011;469(1):69-75. doi:10.1007/s11999-010-1516-0
 29. Sponer P, Korbelt M, Kucera T. Total Knee Arthroplasty in Spondyloepiphyseal Dysplasia with Irreducible Congenital Dislocation of the Patella: Case Report and Literature Review. *Ther Clin Risk Manag*. 2021;17:275-283. doi:https://doi.org/10.2147/TCRM.S294876
 30. Jacquet C, Chan-Yu-Kin J, Sharma A, Argenson JN, Parratte S, Ollivier M. "More accurate correction using "patient-specific" cutting guides in opening wedge distal femur varization osteotomies. *Int Orthop*. 2019;43(10):2285-2291. doi:10.1007/S00264-018-4207-1/TABLES/4
 31. Dasari SP, Hevesi M, Mameri E, et al. Patient-specific instrumentation for medial opening wedge high tibial osteotomies in the management of medial compartment osteoarthritis yields high accuracy and low complication rates: A systematic review. *J ISAKOS*. 2023;8(3):163 – 176. doi:10.1016/j.jisako.2023.02.001
 32. Newclip. Newclip Techniques ActiveMotion S. <https://newcliptechnics.com/lower-limb/osteotomy/activmotion-s/>. Published 2022. Accessed October 28, 2022.
 33. Zhang L, Liu G, Han B, et al. Knee Joint Biomechanics in Physiological Conditions and How Pathologies Can Affect It: A Systematic Review. *Appl Bionics Biomech*. 2020;2020. doi:10.1155/2020/7451683
 34. Niemeyer P, Schmal H, Hauschild O, Von Heyden J, Sdkamp NP, Kstler W. Open-Wedge Osteotomy Using an Internal Plate Fixator in Patients With Medial-Compartment Gonarthrosis and Varus Malalignment: 3-Year Results With Regard to Preoperative Arthroscopic and Radiographic Findings. *Arthrosc J Arthrosc Relat Surg*. 2010;26(12):1607-1616. doi:10.1016/J.ARTHRO.2010.05.006
 35. MacLeod AR, Mandalia VI, Mathews JA, Toms AD, Gill HS. Personalised 3D Printed High Tibial Osteotomy Achieves a High Level of Accuracy: 'IDEAL' Preclinical Stage Evaluation of a Novel Patient Specific System. *Med Eng Phys*. 2022;108:103875. doi:10.1016/J.MEDENGGPHY.2022.103875
 36. Frost HM. Wolff's Law and bone's structural adaptations to mechanical usage: an overview for clinicians. *Angle Orthod*. 1994;64(3):175-188. doi:10.1043/0003-3219
 37. Cross MJ, Spycher J. Cementless fixation techniques in joint replacement. *Jt Replace Technol*. January 2008:190-211. doi:10.1533/9781845694807.2.190
 38. MacLeod AR, Serranoli G, Fregly BJ, Toms AD, Gill HS. The effect of plate design, bridging span, and fracture healing on the performance of high tibial osteotomy plates an experimental and finite element study. *Bone Jt Res*. 2018;7(12):639-649. doi:10.1302/2046-3758.712.BJR-2018-0035.R1/ASSET/IMAGES/LARGE/2046-3758.712.BJR-2018-0035.R1-FIG10.JPEG
 39. Koh YG, Son J, Kim HJ, et al. Multi-objective design optimization of high tibial osteotomy for improvement of biomechanical effect by using finite element analysis. *J Orthop Res*. 2018;36(11):2956-2965. doi:10.1002/JOR.24072
 40. Panagiotis M. Classification of non-union. *Injury*. 2005;36 Suppl 4(SUPPL. 4). doi:10.1016/J.INJURY.2005.10.008
 41. Willemsen K, Nizak R, Noordmans HJ, Castelein RM, Weinans H, Kruyt MC. Challenges in the design and regulatory approval of 3D-printed surgical implants: a two-case series. *Lancet Digit Heal*. 2019;1(4):e163-e171. doi:https://doi.org/10.1016/S2589-7500(19)30067-6
 42. Merema BJ, Kraeima J, ten Duis K, et al. The design, production and clinical application of 3D patient-specific implants with drilling guides for acetabular surgery. *Injury*. 2017;48(11):2540-2547. doi:10.1016/j.injury.2017.08.059
 43. Ijpmma FFA, Meesters AML, Merema BBJ, et al. Feasibility of Imaging-Based 3-Dimensional Models to Design Patient-Specific Osteosynthesis Plates and Drilling Guides. *JAMA Netw Open*. 2021;4(2):e2037519-e2037519. doi:10.1001/JAMANETWORKOPEN.2020.37519
 44. Assink N, Oldhoff MGE, ten Duis K, et al. Development of patient-specific osteosynthesis including 3D-printed

- drilling guides for medial tibial plateau fracture surgery. *Eur J Trauma Emerg Surg*. June 2023;1-9. doi:10.1007/S00068-023-02313-W/TABLES/2
45. MacLeod AR, Peckham N, Serrancolí G, et al. Personalised high tibial osteotomy has mechanical safety equivalent to generic device in a case-control in silico clinical trial. *Commun Med* 2021 11. 2021;1(1):1-9. doi:10.1038/s43856-021-00001-7
 46. Kanagalingam S, Dalton C, Champneys P, et al. Detailed design for additive manufacturing and post processing of generatively designed high tibial osteotomy fixation plates. *Prog Addit Manuf*. October 2022:1-18. doi:10.1007/S40964-022-00342-2/FIGURES/19
 47. McKnight M. Generative Design: What it is? How is it Being Used? Why it's a Game Changer! In: *The International Conference on Design and Technology*. ; 2017:176-181. doi:10.18502/keg.v2i2.612
 48. Yang W fa, Choi WS, Wong MCM, et al. Three-Dimensionally Printed Patient-Specific Surgical Plates Increase Accuracy of Oncologic Head and Neck Reconstruction Versus Conventional Surgical Plates: A Comparative Study. *Ann Surg Oncol*. 2021;28(1):363. doi:10.1245/S10434-020-08732-Y
 49. Takizawa T, Nakayama N, Haniu H, et al. Titanium Fiber Plates for Bone Tissue Repair. *Adv Mater*. 2018;30(4). doi:10.1002/ADMA.201703608
 50. Yoo OS, Lee YS, Lee MC, Elazab A, Choi DG, Jang YW. Evaluation of the screw position and angle using a post-contoured plate in the open wedge high tibial osteotomy according to the correction degree and surgical technique. *Clin Biomech*. 2016;35:111-115. doi:10.1016/J.CLINBIOMECH.2016.04.016
 51. Stoffel K, Dieter U, Stachowiak G, Gächter A, Kuster MS. Biomechanical testing of the LCP - How can stability in locked internal fixators be controlled? *Injury*. 2003;34(SUPPL. 2). doi:10.1016/J.INJURY.2003.09.021
 52. Gautier E, Sommer C. Guidelines for the clinical application of the LCP. *Injury*. 2003;34(SUPPL. 2):63-76. doi:10.1016/J.INJURY.2003.09.026
 53. Koh YG, Lee JA, Lee HY, Chun HJ, Kim HJ, Kang KT. Design optimization of high tibial osteotomy plates using finite element analysis for improved biomechanical effect. *J Orthop Surg Res*. 2019;14(1):1-10. doi:10.1186/S13018-019-1269-8/FIGURES/8
 54. Röderer G, Gebhard F, Duerselen L, Ignatius A, Claes L. Delayed bone healing following high tibial osteotomy related to increased implant stiffness in locked plating. *Injury*. 2014;45(10):1648-1652. doi:10.1016/J.INJURY.2014.04.018
 55. Nakamura R, Akiyama T, Takeuchi R, Nakayama H, Kondo E. Medial Closed Wedge Distal Femoral Osteotomy Using a Novel Plate With an Optimal Compression System. *Arthrosc Tech*. 2021;10(6):e1497-e1504. doi:10.1016/J.EATS.2021.02.016
 56. Sonderegger J, Grob KR, Kuster MS. Dynamic plate osteosynthesis for fracture stabilization: how to do it. *Orthop Rev (Pavia)*. 2010;2(1):4. doi:10.4081/OR.2010.E4
 57. Bliven EK, Greinwald M, Hackl S, Augat P. External fixation of the lower extremities: Biomechanical perspective and recent innovations. *Injury*. 2019;50:S10-S17. doi:10.1016/J.INJURY.2019.03.041
 58. Wähnert D, Windolf M, Brianza S, et al. A comparison of parallel and diverging screw angles in the stability of locked plate constructs. *J Bone Jt Surg - Ser B*. 2011;93 B(9):1259-1264. doi:10.1302/0301-620X.93B9.26721/ASSET/IMAGES/LARGE/26721-GALLEYFIG9.JPG
 59. Cheng CT, Luo CA, Chen YC. Biomechanical effects of screw orientation and plate profile on tibial condylar valgus osteotomy - Finite-element analysis. <https://doi.org/10.1080/1025584220201772763>. 2020;23(12):906-913. doi:10.1080/10255842.2020.1772763
 60. Luo CA, Lin SC, Hwa SY, Chen CM, Tseng CS. Biomechanical effects of plate area and locking screw on medial open tibial osteotomy. <http://dx.doi.org/10.1080/102558422014895335>. 2014;18(12):1263-1271. doi:10.1080/10255842.2014.895335
 61. Bel JC. Pitfalls and limits of locking plates. *Orthop Traumatol Surg Res*. 2019;105(1):S103-S109. doi:10.1016/J.OTSR.2018.04.031
 62. Kiyono M, Noda T, Nagano H, et al. Clinical outcomes of treatment with locking compression plates for distal femoral fractures in a retrospective cohort. *J Orthop Surg Res*. 2019;14(1):1-9. doi:10.1186/S13018-019-1401-9/TABLES/5
 63. Ahmad M, Nanda R, Bajwa AS, Candal-Couto J, Green S, Hui AC. Biomechanical testing of the locking compression plate: When does the distance between bone and implant significantly reduce construct stability? *Injury*. 2007;38(3):358-364. doi:10.1016/J.INJURY.2006.08.058
 64. Yang JCS, Lin KP, Wei HW, et al. Importance of a moderate plate-to-bone distance for the functioning of the far cortical locking system. *Med Eng Phys*. 2018;56:48-53. doi:10.1016/J.MEDENGGPHY.2018.04.006
 65. Davis JR. *Metals Handbook Desk Edition*. 2nd editio. ASM International; 1998.
 66. Taylor WR, Heller MO, Bergmann G, Duda GN. Tibio-femoral loading during human gait and stair climbing. *J Orthop Res*. 2004;22(3):625-632. doi:10.1016/J.ORTHRES.2003.09.003
 67. Schröter S, Ateschrang A, Löwe W, Nakayama H, Stöckle U, Ihle C. Early full weight-bearing versus 6-week partial weight-bearing after open wedge high tibial osteotomy leads to earlier improvement of the clinical

- results: a prospective, randomised evaluation. *Knee Surg Sports Traumatol Arthrosc.* 2017;25(1):325-332. doi:10.1007/S00167-015-3592-X
68. Pereira T, Kennedy J V., Potgieter J. A comparison of traditional manufacturing vs additive manufacturing, the best method for the job. *Procedia Manuf.* 2019;30:11-18. doi:10.1016/J.PROMFG.2019.02.003
69. Davis R, Singh A, Jackson MJ, et al. A comprehensive review on metallic implant biomaterials and their subtractive manufacturing. *Int Journal, Adv Manuf Technol.* 2022;120(3-4):1473. doi:10.1007/S00170-022-08770-8
70. Evans R. Selection and testing of metalworking fluids. *Metalwork Fluids Cut Grind Fundam Recent Adv.* January 2012:23-78. doi:10.1533/9780857095305.23
71. Ahmad M, Nanda R, Bajwa AS, Candal-Couto J, Green S, Hui AC. Biomechanical testing of the locking compression plate: when does the distance between bone and implant significantly reduce construct stability? *Injury.* 2007;38(3):358-364. doi:10.1016/J.INJURY.2006.08.058
72. Kandemir U, Herfat S, Herzog M, Viscogliosi P, Pekmezci M. Fatigue Failure in Extra-Articular Proximal Tibia Fractures: Locking Intramedullary Nail Versus Double Locking Plates-A Biomechanical Study. *J Orthop Trauma.* 2017;31(2):e49-e54. doi:10.1097/BOT.0000000000000729
73. Zhang LC, Chen LY. A Review on Biomedical Titanium Alloys: Recent Progress and Prospect. *Adv Eng Mater.* 2019;21(4):1801215. doi:10.1002/ADEM.201801215

Appendix A. Background Literature Design Requirements

While adequate stabilization is crucial, achieving a balance between rigidity and IFM is of high importance to stimulate bone healing and prevent fatigue failure. This balance depends on various design characteristics related to screw type and position, shape, material, and production process of the plate. These characteristics and its effects are identified in literature and described here, forming the basis of the design requirements. To translate this theoretical framework into a design with specific values, measurements were conducted on certified generic osteotomy plates. These measurements include the distance between proximal screws, the spacing and orientation of the distal screws, the bridging span and the distance between screws and the edge of the plate.

Type and number of screws

Traditionally, for plate fixation in osteotomy, three to four screws are inserted at each fragment^{39,50}. In theory, two or three screws on either side of the fracture should be sufficient to stabilize fractures of the lower extremity. Previous research has demonstrated that using more than three screws has a minimal impact on increasing axial stiffness, and employing four screws does not significantly enhance torsional rigidity.⁵¹ However, such a construct can only be used in good bone quality and when the surgeon is sure that all the screws are inserted correctly and bicortically. Therefore, in clinical guidelines a minimum of three locking screws is recommended.⁵² Additional to the locking screws, a compression screw can be inserted in a ramp oblong hole perpendicular and proximal to the oblique osteotomy line. This allows for a simple and controlled compression by the screw-plate interface.^{32,55}

The use of locking screws reduces the average stress on the bone compared to compression screws, but it results in a higher average stress on the plate. Locking plates are associated with high rigidity, which can cause stress shielding.^{53,54}

Screw position

Optimal screw position leads to load-sharing between the bone, plate, and screws, eliminating stress shielding³⁹. It has been demonstrated that lag screws, traditionally used to compress fracture fragments, reduce motion at the fracture gap dramatically and screws close to the fracture site must be avoided whenever possible.⁵⁶

Proximal screws are placed parallel to each other in axial direction, as diverging screw angles show a biomechanical disadvantage under static and cyclical loading⁵⁸. Distal screws can only be placed unicortical, resulting in decreased bone anchoring, compression and torsional resistance, and breaking load. The decrease is especially in osteoporotic bone as the cortex gets thinner.⁶¹ Divergent and convergent screw direction enhances the pullout strength of the screws⁵². Research suggests that divergent screw direction increases construct stability which can decrease fracture risk in screws, plate and bone, allowing the smallest IFM⁵⁹.

The distance between the screws on either side of the osteotomy line, referred to as the bridging span, has a major impact on the balance between stability and IFM. Screw insertions near the fracture site increase fracture stability⁶², while larger bridging spans in opening wedge HTO increase IFM without substantially increasing plate stress³⁸. When an external load is applied to the bone-plate construct, the plate will most likely bend at the height of the bridging span. Bending a plate over a short segment enhances the local strain of the implant, while bending over a longer segment reduces the local strain, resulting in a protective effect against fatigue failure of the implant⁵². In guidelines for locking plates with a gap size of 1 mm, it is recommended to omit at least one hole on each side of a fracture⁵¹. The length of the bridging span for the generic DFO plate is 25 mm.

Plate

A study examining the mechanical stability of an LCP construct in a simulated diaphyseal fracture found that plate-bone distance should be equal to or less than 2 mm.⁶³ When applied 5 mm from the bone, the plate demonstrated significantly increased plastic deformation during cyclical compression and required lower loads to induce construct failure. Moreover, a plate-bone distance of 2 mm had the advantages of reducing axial stiffness and providing nearly parallel IFM⁶⁴. By increasing this distance from 2 mm to 6 mm, both torsional rigidity and axial stiffness decreased by 10-15%⁵¹, which is consistently associated with reduced fatigue life^{71,72}. In a biomechanical study that compared the effects of contoured plate profile compared to straight design bridging an off-set, an increased fracture risk of screw, plate, and bone was observed at 7.7%, and 4.3% and 7.9%, respectively. ⁵⁹

Ti6Al4V is an alpha-beta alloy and the most widely used as biomechanical implants due to its high specific strength, lower elastic modulus, excellent biocompatibility, and enhanced corrosion resistance. Nevertheless, there are still some problems with the long-term performance of titanium alloys, related to biological activity, wear resistance, and corrosion resistance. Such problems are often restricted by the surface properties of the implants, hence various surface modification methods have been employed.⁷³

Appendix B. Theory Simple Bending of a Beam

The bending behavior of a curved plate can be estimated by comparing it to simple bending of a beam. The maximal bending stress in a beam under simple bending, with M is the bending moment at location of interest along the beam length, c is the centroidal distance of the cross section, and I_c is the centroidal moment of inertia of the beam's cross section.

$$\sigma_{b.max} = \frac{M \cdot c}{I_c}$$

In a simple beam, the distance to the neutral axis is equal to the height of the beam divided by two. The cross section of the plate is simplified as a rectangular section, for which the moment of inertia $I = w \cdot t^2 / 12$, with w the width and t the thickness of the beam. As the thickness of the beam can be compared to the thickness of the plate, the maximum stress in the plate can be estimated, depending on the curve and thickness of the plate.

$$\sigma_{b.max} = \frac{M \cdot \frac{t}{2}}{\frac{1}{12} \cdot w \cdot t^3} = \frac{6 \cdot M}{w} \cdot \frac{1}{t^2}$$

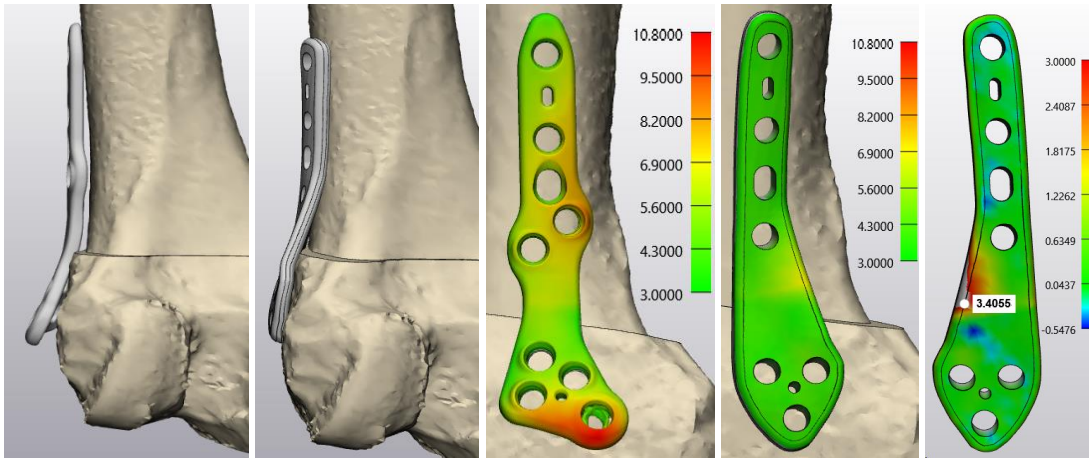
Or, in other words, given a certain bending moment M and width b of a beam, the ratio between max. stress and squared thickness of the beam is constant:

$$\sigma_{b.max} \cdot t^2 = \frac{M}{w} = \text{constant}$$

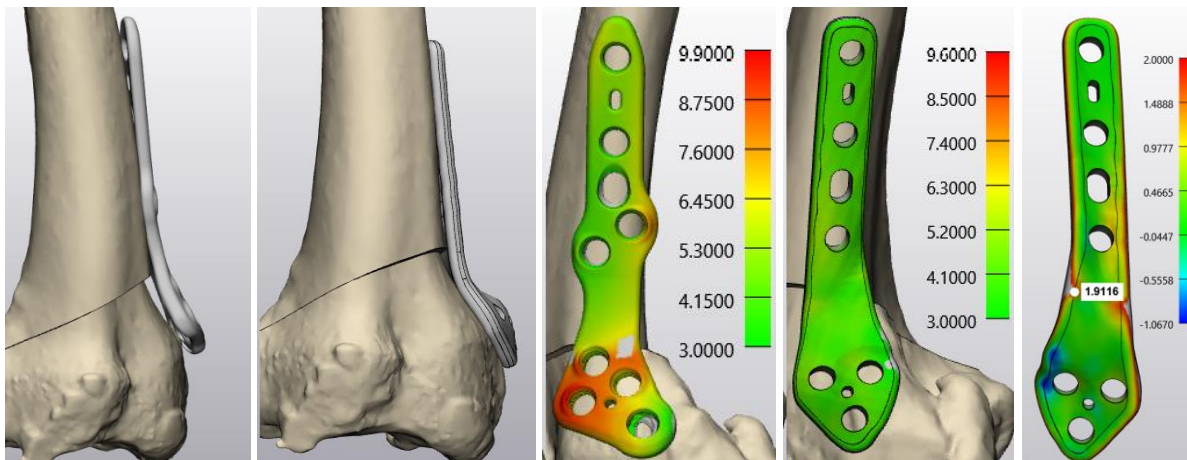
Appendix C. Virtual Validation Analysis

A virtual distal femur osteotomy was conducted on five patients, and the femur was fixated using both a generic plate and a patient-specific plate. This appendix includes images displaying a side view of the plate for visual inspection of the fitting and longitudinal curve, as well as a front view with measurements of the plate-bone distance.

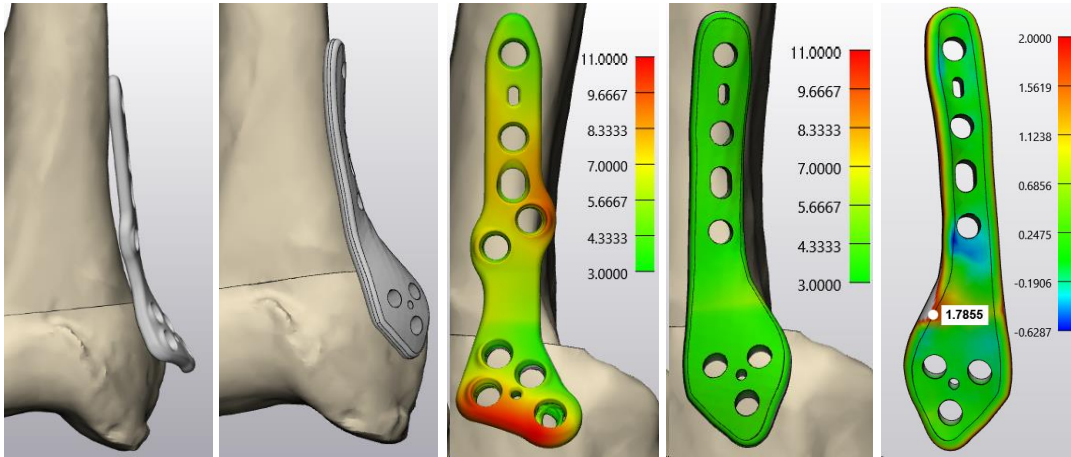
Patient 1.



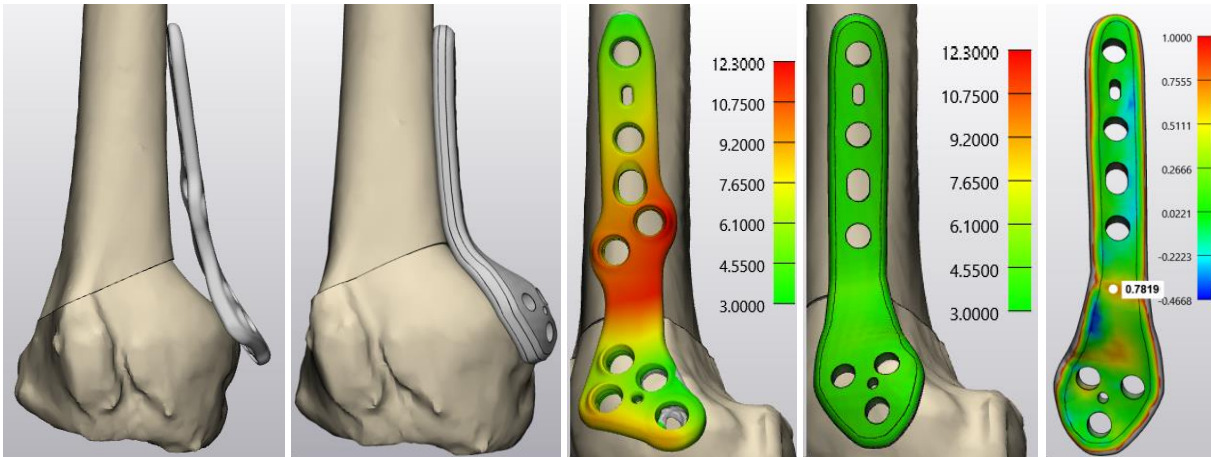
Patient 2.



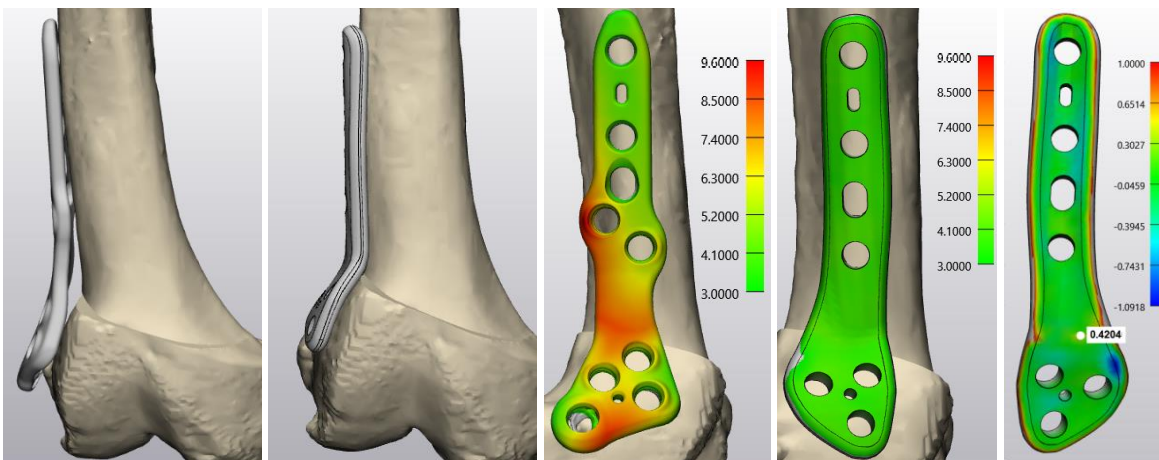
Patient 3.



Patient 4.



Patient 5.



Appendix D. Risk Analysis: Potential Modes of Failure

Potential modes of failure are identified throughout the design phase, manufacturing, per-operative, and post-operative phases. For each mode of failure, potential consequences and corresponding measurements to prevent them are determined.

To assess whether the residual risk is acceptable, scores were assigned to the likelihood of occurrence and the severity of consequences, following the values provided in Table D1. Using these scores, a risk score is calculated by multiplying the likelihood of occurrence by the severity value. Subsequently, the risk score can be categorized into four levels, as outlined in Table D2.

Table D1: Quantification of the likelihood of occurrence and the severity of the consequences

Likelihood of occurrence	Likelihood value	Severity	Severity value
Daily	10	Invalidity	10
Weekly	9	Death	9
Monthly	8	Permanent injury	8
Yearly	7	Reversible injury	7
Less than once a year	6	No injury	6

Table D2: Classification of the risk score

Risk score	Value	Color coding	Action
Very low	< 50	Green	Risk is acceptable
Low	50-69	Yellow	Risk reduction is required
High	70-79	Orange	
Very high	> 80	Red	Risk is unacceptable

Potential mode of failure	Consequence	Likelihood occurrence (Before implementing)	Severity	Risk score	Measures to be taken	Likelihood occurrence (After implementing measures)	Severity	Risk score	Residual risk	
Product Design										
The product is designed in such a way that cleaning and sterilization are not straightforward, leaving residue The plate is designed in a way that it cannot be properly placed on the femur or screws cannot be placed The plate design does not align with the pre-drilled screw holes guided by the PSI The plate is not applicable as intended by the physician (poor communication between 3D-lab and physician)	Plate might be unsterile or residue is left in the patient	Yearly	Permanent injury	56	Check the design for angles that cannot be cleaned or sterilized	Less than once a year	Permanent injury	8	48	Very low
	Operation must proceed with a generic plate	Less than once a year	Reversible injury	42	The surgery is practiced on a nylon 3D printed bone model, PSI and plate	Less than once a year	Reversible injury	7	42	Very low
	Extra screw holes need to be drilled, or the operation must proceed with a generic plate and Operation must proceed with a generic plate	Yearly	Reversible injury	49	Surgeons are trained to perform the surgery with a generic plate.	Less than once a year	Reversible injury	7	42	Very low
		Less than once a year	No injury	36	The surgeon's signature is required for the order file to gain early insight into the design	Less than once a year	No injury	6	36	Very low
Manufacturing										
An error occurs during finishing	Biocompatible properties and mechanical safety are not	Less than once a year	Permanent injury	48	Surgeons are trained to perform the surgery with a generic plate.	Less than once a year	Permanent injury	8	48	Very low
The plate is damaged during finishing	Operation must be postponed or must proceed with a generic	Less than once a year	No injury	36	Surgeons are trained to perform the surgery with a generic plate.	Less than once a year	No injury	6	36	Very low
Usage										
The plate is not available on time	Operation must be postponed or must proceed with a generic plate	Less than once a year	No injury	36	Clear user manual - for complex cases, the 3D expert is present in the operating room.	Less than once a year	No injury	6	36	Very low
The plate is found not to fit well on the femur during the operation	Operation must proceed with a generic plate	Yearly	No injury	42	The surgery is practiced on a nylon 3D printed bone model, PSI and plate	Less than once a year	No injury	6	36	Very low
Facilities (ICT/sterilization)										
Incorrect sterilization method is applied to the plate	Damage or deformation of the plate	Less than once a year	Permanent injury	48	Ensure that surgeons are trained to perform the surgery with a generic plate.	Less than once a year	Permanent injury	8	48	Very low
Software malfunctions or crashes	The plate cannot be designed according to the design workflow, or not at all	Less than once a year	No injury	36	Ensure that surgeons are trained to perform the surgery with a generic plate.	Less than once a year	No injury	6	36	Very low
An outdated version of the CAD/CAM software is used	Possible new improved functionalities are not implemented	Yearly	No injury	42	Ensure that there are fixed moments in the year when packages are checked, and making sure that suppliers inform us of updates.	Less than once a year	No injury	6	36	Very low
For implants (medical device remains inside the patient)										
The implant cannot be removed when necessary	Surrounding bone structure must be removed along with the implant during removal	Yearly	Permanent injury	56	Make the plate out of titanium alloy, round the edges of the design, low profile design.	Less than once a year	Permanent injury	8	48	Very low
The plate experiences mechanical failure	The plate must be removed and replaced if the bone parts are not consolidated	Yearly	Permanent injury	56	Adjusting the thickness of the plate, so that the stress in the plate is similar to, or smaller than, the stress in a generic plate under the same loading	Less than once a year	Permanent injury	8	48	Very low